

Critical exponents of a three dimensional weakly diluted quenched Ising model

R. Folk⁽¹⁾, Yu. Holovatch^(2,3), T. Yavors'kii⁽³⁾

⁽¹⁾Institut für theoretische Physik, Johannes Kepler Universität Linz, A-4040 Linz, Austria

E-mail: folk@tphys.uni-linz.ac.at

⁽²⁾Institute for Condensed Matter Physics, National Academy of Sciences of Ukraine, UA-79011 Lviv, Ukraine

E-mail: hol@icmp.lviv.ua

⁽³⁾Ivan Franko National University of Lviv, UA-79005 Lviv, Ukraine

E-mail: tarasyk@ktf.franko.lviv.ua

(April 26, 2024)

We discuss universal and non-universal critical exponents of a three dimensional Ising system in the presence of weak quenched disorder. Both experimental, computational, and theoretical results are reviewed. Special attention is paid to the results obtained by the field theoretical renormalization group approach. Different renormalization schemes are considered putting emphasis on analysis of divergent series obtained.

Key words: critical phenomena, quenched disorder, Ising model.

PACS numbers: 64.60.Ak, 61.43.-j, 11.10.Gh

I. INTRODUCTION

The present paper reviews properties of a three-dimensional weakly diluted quenched Ising model (random Ising model: RIM – see figure 1) in the vicinity of critical point. For weak dilution by a non-magnetic component, i.e. far from the percolation threshold, the magnetic second-order phase transition still maintains in the RIM [1] although it possesses novel features in comparison with the pure $d = 3$ Ising model. Static critical exponents of a RIM [3] have been a subject of a detailed experimental [4–20], numerical [21–40] and theoretical [42–65] analysis almost for three decades. Recently, new data were obtained both in experimental measurements [15–20] and Monte Carlo simulations [33–40]. Theoretical breakthrough occurred along several months in 1999–2000 when the perturbation expansion series for RIM were extended from the 4th [54] through 5th [63,64] to the sixth order [66,65]. Therefore it seems for us worth collecting together the bulk of available results concerning critical behaviour of the RIM.

In the present discussion, we will be mainly interested in the RIM critical exponents. An *asymptotic critical exponent* x of a physical observable $\mathcal{O}(\tau)$ is defined [67] asymptotically close to the critical point T_c : $x \equiv \lim_{\tau \rightarrow 0} \frac{\ln \mathcal{O}(\tau)}{\ln |\tau|}$, where $\tau = (T - T_c)/T_c$ is the reduced distance to the critical point. For instance, the magnetic susceptibility χ diverges as:

$$\chi \simeq \Gamma_{\pm} |\tau|^{-\gamma}, \quad \tau \rightarrow 0 \quad (1)$$

where γ is the susceptibility critical exponent, while Γ_+ and Γ_- are critical amplitudes above and below the critical point respectively. The power law of type (1) holds exactly in the asymptotic regime $\tau \rightarrow 0$. In this regime the critical exponents and ratios of the critical amplitudes take constant values. According to the universality hypothesis they are defined by global variables only. For a short-range interaction the global variables are the space dimension and tensor characteristics of an order parameter. In the non-asymptotic regime the approach to criticality is described by non-universal *effective critical exponents*, which are introduced to describe the behaviour of a quantity in a certain temperature interval [68,69]. The susceptibility effective critical exponent γ_{eff} by definition reads:

$$\gamma_{eff}(\tau) = \frac{d \ln \chi(\tau)}{d \ln \tau}. \quad (2)$$

In the asymptotic limit $\tau \rightarrow 0$ the effective and asymptotic exponents coincide. In the intermediate region the behaviour is characterized by the so-called Wegner expansion [70]:

$$\chi \simeq \Gamma_{\pm} |\tau|^{-\gamma} (1 + \Gamma_{1,\pm} |\tau|^{\omega\nu} + \Gamma_{2,\pm} |\tau|^{2\omega\nu} + \dots), \quad (3)$$

where $\Gamma_{1,\pm}, \Gamma_{2,\pm}$ are non-universal amplitudes, ν is the correlation length critical exponent, and ω is the correction-to-scaling exponent.

It is the art of a physicist which allows to discriminate between regimes (1)–(3) either performing experimental measurements or doing theoretical calculations and numerical simulations. Below we will review available data on effective and asymptotic critical exponents of the RIM. The paper is arranged as follows. In the next section II we

will give general considerations about an influence of a weak quenched disorder on a second order phase transition, formulate the model as well as outline the main features of its critical behaviour. In Section III we review experiments on weakly diluted uniaxial magnets, whereas computer Monte Carlo simulations of a RIM are analyzed in Section IV. In sections V and VI we outline the method of renormalization group as the most fruitful theoretical tool in the study of the critical properties of RIM. We consider different renormalization schemes and pay special attention to analysis of divergent series obtained within the approach. Conclusions (Section VII) complete the article.

II. WEAKLY DILUTED QUENCHED ISING MODEL

The central questions one has to answer studying the influence of weak disorder on a magnetic second-order phase transitions are: do the critical exponents of a homogeneous magnet change under dilution by a non-magnetic component? And if this is the case, are the new exponents universal? Regarding the first question it was argued [71] that if the heat capacity critical exponent α of the pure (undiluted) system is positive, i.e. the heat capacity diverges at the critical point, then a quenched disorder causes changes in the critical exponents. This statement is known as Harris criterion. Later, for a large class of d -dimensional disordered systems it was proven that the correlation length critical exponent ν must satisfy the bound $\nu \geq 2/d$ [72]. Both statements focus attention towards studies of the $d = 3$ Ising model, where the typical numerical values of the above exponents, together with the magnetic susceptibility and the order parameter critical exponents in the pure case read [73]:

$$\alpha = 0.109 \pm 0.004 > 0, \nu = 0.6304 \pm 0.0013 < 2/3, \gamma = 1.2396 \pm 0.0013, \beta = 0.3258 \pm 0.0014. \quad (4)$$

According the inequalities of the criteria mentioned above for the case of the diluted Ising model new exponents are expected.

In order to obtain precise values of critical exponents it is standard now to rely on renormalization group methods. In particular, the theoretical estimates given above (4) were obtained on the basis of a deep analogy between long-distance properties of the Ising model in the neighbourhood of a second-order phase transition point and a field theory with an effective Landau-Ginzburg-Wilson Hamiltonian of the form:

$$\mathcal{H}_{\text{Ising}}(\varphi) = \int d^3R \left\{ \frac{1}{2} [|\nabla\varphi|^2 + m_0^2\varphi^2] + \frac{\tilde{u}_0}{4!} \varphi^4 \right\}, \quad (5)$$

where m_0^2 is a bare mass proportional to distance to a critical point, $\varphi = \varphi(R)$, \tilde{u}_0 are (bare) scalar field and coupling.

One of the ways to introduce quenched dilution to the effective Hamiltonian (5) is to add to m_0^2 the random-temperature like variable [45] $\psi = \psi(R)$:

$$\mathcal{H}_\psi(\varphi) = \int d^3R \left\{ \frac{1}{2} [|\nabla\varphi|^2 + (m_0^2 + \psi)\varphi^2] + \frac{\tilde{u}_0}{4!} \varphi^4 \right\}. \quad (6)$$

Taking that ψ obeys Gaussian distribution:

$$P(\psi) = \frac{1}{\sqrt{4\pi w}} \exp(-\psi^2/4w^2) \quad (7)$$

with w^2 being a half of dispersion, and introducing n replicas [75] of a model (5) in order to perform averaging over quenched disorder [76] one ends up [45] with a familiar effective Hamiltonian:

$$\mathcal{H}_{\text{RIM}}(\varphi) = \int d^3R \left\{ \frac{1}{2} \sum_{\alpha=1}^n [|\nabla\varphi_\alpha|^2 + m_0^2\varphi_\alpha^2] + \frac{u_0}{4!} \sum_{\alpha=1}^n \varphi_\alpha^4 + \frac{v_0}{4!} \left(\sum_{\alpha=1}^n \varphi_\alpha^2 \right)^2 \right\}. \quad (8)$$

In the limit $n \rightarrow 0$ field theory (8) describes critical properties of a RIM. Here, the bare coupling u_0 is positive (being proportional to \tilde{u}_0) whereas the bare coupling v_0 is proportional to minus variance of the random variable ψ and thus is negative. The last term in (8) is present only for non-zero dilution: it is directly responsible for the fluctuations effective interaction due to the presence of impurities.

Often (e.g. in Monte Carlo simulations) the microscopic Hamiltonian of RIM is written in the following form:

$$H = -\frac{1}{2} \sum_{R,R'} J(|R - R'|) S_R S_{R'} c_R c_{R'}, \quad (9)$$

where R runs over sites of simple cubic lattice, J is a short-range translationally invariant interaction between pairs of $S = \pm 1$ “classical” Ising spins, c_R is an occupation number equal either to 0 or to 1. It is considered that geometrically the vacancies $c_R = 0$ are distributed independently according to the law

$$P(c_R) = (1 - p)\delta(c_R) + p\delta(1 - c_R) \quad (10)$$

and fixed in different sites of the lattice (see figure 1). In (10) $p \leq 1$ is the concentration of occupied sites. Calculating free energy of a model (9) and using replica trick [75] to perform the configurational averaging of the logarithm of configuration-dependent partition function it is straightforward to show that one ends up with the effective Hamiltonian of (8) type in the $n \rightarrow 0$ replica limit with $u_0 \sim p$ and $v_0 \sim p(p - 1)$.

From the viewpoint of dynamics one can point to two opposite types of a disorder [3]. If a characteristic time of impurities dynamics is comparable to relaxation times in the pure system, impurity variables are treated identically to the “pure” dynamical variables and are a part of the disordered system phase space. The corresponding annealed disorder [76] is a subject of special investigations and reveals trivial results at criticality. The so called Fisher renormalization [77] states that when a heat capacity critical exponent of an undiluted system α_{pure} is positive, then the critical exponents x of an annealed system are determined by those of the corresponding pure one (x_{pure}) by a simple renormalization of the form:

$$x = \frac{x_{pure}}{1 - \alpha_{pure}}, \quad \alpha = \frac{-\alpha_{pure}}{1 - \alpha_{pure}}. \quad (11)$$

This explains why prevailing interest is attracted by the quenched disorder when impurities can be considered as fixed and thus one needs to perform configurational average over an ensemble of disordered systems with different realization of the disorder.

The Hamiltonian (8) represents critical properties of the problem (9) for small randomness. Alternatively, the scale-invariant fractal ramified cluster at the percolation threshold is a starting point of the strong disorder approach. Here, the field theoretical description starts with the effective Hamiltonian of the Potts model. A unified theory of random systems critical behaviour which would give both regimes of strong disorder and weak disorder as its limiting cases is still absent.

The translation invariant Hamiltonian (8) presumes perturbative account of thermal fluctuations around a spatially homogeneous unique ground state. While it appears to hold for a pure system, for a random system there is a macroscopic number of spatially inhomogeneous ground states in a disorder dominated region. These correspond to local minimum solutions of a saddle-point equation for the effective Hamiltonian (8) [78,79]. Physically the last corresponds to the so-called Griffiths phase [80] caused by the existence of ferromagnetically ordered “islands” in the temperature interval between the critical temperatures of pure and random systems. The description of the phase at the critical point is provided by a replica-symmetry breaking Hamiltonian [78] leading to non-trivial results [81,82]. However recently a refined analysis of the problem brought about a stability of the critical behaviour of the weakly disordered systems with respect to replica symmetry breaking effects [83]. The theoretical results reviewed in the present discussion will be based on the replica symmetrical Hamiltonian (8) (see section V).

The effective Hamiltonians (6) and (8) possess different global variables: although the space dimension is the same ($d = 3$) the symmetry and order parameter components number differ. Thus one may expect that by application of renormalization group approach they will lead to different critical behaviour. One of the central notions in the renormalization group formalism applied to the critical phenomena is the notion of the fixed point of the renormalization group transformation. If a fixed point exists and it can be reached from the initial values of the couplings it corresponds to a critical point of the system. Applying the renormalization group transformation to the effective Hamiltonian (6) and starting from positive values of u one reaches the stable fixed point u^* which corresponds to the critical point of a $d = 3$ pure Ising model and leads in particular to the results (4). The fixed point structure for the effective Hamiltonian (8) is sketched in figure 2. The earliest qualitative results about the structure of RIM fixed points appeared in mid-seventies [43–45]. Later analysis supported this picture [48,50,84]: indeed the fixed point **I** of the $d = 3$ pure Ising model appears to be unstable and a new stable fixed point **R** exists (see figure 2). Thus the general answer of the renormalization group analysis of the RIM supports non-perturbative results of Refs [71,72]: RIM critical behaviour is governed by critical exponents different from those of the pure Ising model.

In the subsequent chapters we will have a look how this statement was made clear in experimental, Monte Carlo and theoretical studies.

III. EXPERIMENTAL STUDY

The Ising model is represented in experiments on magnets by crystalline difluoride of a transition metal, normally iron or manganese. In FeF_2 which possesses a rutile crystalline structure with $a = 4.697\text{\AA}$ and $c = 3.309\text{\AA}$ at room

temperature [85], the spins of metal ions align along c axis in such a way that spins of the body-centered ions are oriented in opposite directions to those of the corner ions. The system can be well described by a Heisenberg-like spin $S = 2$ Hamiltonian with quadratic anisotropic single ion terms and other interactions less than 6% of interspin exchange force constant $J = 0.45$ meV, as follows from the spin-wave dispersion relations on the basis of neutron scattering measurements [86]. Dominant intersublattice exchange interaction and high anisotropy makes FeF_2 a very good experimental realization of an Ising antiferromagnet, where the order parameter is the sublattice magnetization. Experimental studies confirm pure Ising model critical behaviour for the reduced temperature range $|\tau| < 10^{-1}$ ($\tau \equiv (T - T_N)/T_N$) around Néel temperature T_N . Another example is MnF_2 with similar crystalline structure but much weaker single ion anisotropy than FeF_2 , however the experimental study showed the substance to belong to the Ising universality class [87–89] as well.

A material which corresponds to RIM can be obtained as a crystalline mixture of two compounds on the basis of “pure” Ising model matrix (see Table I). A corresponding site-diluted uniaxial alloy can be prepared by substitution of FeF_2 (MnF_2) with non-magnetic isomorph ZnF_2 . Experiments on the critical behaviour of random systems are extremely sensitive to the sample quality. Asymptotic critical behaviour is observable only very close to T_N and macroscopic non-statistical gradients in concentration cause variation of T_N through the sample smearing out the sharp transition. Therefore, to provide a satisfactory good realization of random substitutional disorder of magnetic ions (Fe^{+2} , Mn^{+2}) by non-magnetic ones (Zn^{+2}), mixed crystals $\text{Fe}_p\text{Zn}_{1-p}\text{F}_2$ as well as $\text{Mn}_p\text{Zn}_{1-p}\text{F}_2$ should be grown with very high crystalline accuracy of the mosaic pattern, chemical homogeneity and especially with small impurity concentration gradients. The last can be achieved by choosing a concentration of impurities such that [91] $dT_N/dp = 0$ or by a geometry which takes into account that usually gradients are parallel to the growth axis. Early experimental studies on the disordered crystals critical behaviour [92,93] proved the crucial role of a sample quality and high quality samples allowed to observe sharp phase transition and to measure the dependence of Néel temperature T_N on p via linear birefringence method [94]. This provided a basis for universal critical properties measurements. The earliest experimental study of the critical exponents governing the sharp transition at a weak quenched dilution was the nuclear magnetic resonance measurement of magnetization in $\text{Mn}_{0.864}\text{F}_{0.136}\text{F}_2$ [4]. The value of magnetization exponent β was found to differ strongly from that in non-diluted sample (see Table I for details).

In a few years the study of Ref. [4] was corroborated by nuclear scattering (NS) measurements in a two-axis spectrometer configuration [5] of the staggered susceptibility and the correlation length in a crystal on the iron basis with concentration $p = 0.5$ in the high dilution regime. In the experiment the smearing effect was eliminated by masking the crystal to expose only a small homogeneous region, while the relative temperature control to about $0.01K$ together with the substance Néel temperature $42.50K$ gave the accuracy $\delta|\tau| \sim 5 \times 10^{-4}$ for reduced temperature. The data for the inverse correlation length and the inverse staggered susceptibility were fit to power laws with critical amplitudes and exponents as free parameters. The power law was shown to be satisfied well within $10^{-3} \div 2 \times 10^{-1}$ with the same critical exponents (see Table I) below and above T_c and differing strongly from those of the pure Ising model. To support the result by alternative experimental methods caloric properties were measured. Utilizing the fact that for transition-metal difluorides the temperature derivative of the linear birefringence is proportional to the magnetic specific heat within [94,95] $|\tau| < 10^{-1}$, measurements of the critical exponent α were performed for a sample $\text{Fe}_{0.6}\text{Zn}_{0.4}\text{F}_2$ with $T_N = 47.05$. In order to minimize the effect of concentration gradients the laser beam was oriented perpendicularly to the concentration gradient. The numerical value of the critical exponent was extracted by fitting the data to the temperature integral of specific heat scaling function taking into account correction-to-scaling terms (i.e. the first two terms in the expansion (3)). In contrast to the pure Ising case, the data obtained yielded $\alpha < 0$ (see Table I). Within no region in reduced temperature τ any evidence of pure Ising behaviour or a crossover from pure to random fixed point critical behaviour was found. So one concluded that the crossover is either outside the critical region or it is too slow. The data obtained in Ref. [5] on the basis of two different substances and quite different experimental procedures proofed that the scaling relation $d\nu = 2 - \alpha$ holds for them and thus supported strongly scaling in dilute systems.

With a typical energy of the neutron beam about 10 meV, the NS measurements appeared to be one of the most useful method to study criticality, however they turned out to be in particular very sensitive to the sample quality since typical sample sizes are less than several millimeters. The NS measurements contain contributions from transverse and longitudinal spin fluctuations, which have to be separated in a detailed data analysis. This explains why in the neutron scattering measurements of the Ref. [7] which were performed on $\text{Fe}_p\text{Zn}_{1-p}\text{F}_2$ with concentration 0.46 on the similar device, special attention was paid to the quality of a sample. In the study a variation 2×10^{-4} in concentration over the entire volume was achieved which permitted scattering studies up to $|\tau| \geq 10^{-3}$. Within the interval $1.5 \times 10^{-3} \leq |\tau| \leq 10^{-1}$ the inverse correlation length was obtained from the width of the Lorentzian fits as a function of temperature, and the correlation length exponent was extracted from the power-law fits. The fit to the power ansatz for χ with background term yielded γ after extrapolation to the wave vector length $q = 0$ (see Table I). An alternative substance with the base Mn ($\text{Mn}_p\text{Zn}_{1-p}\text{F}_2$) was studied by neutron scattering experiments a year later [9]. The sample with $p = 0.75$ had overall spread in concentration 0.001 and allowed to perform measurements up to

$|\tau| \sim 4 \times 10^{-4}$ (see figure 3), while the $p = 0.5$ sample was of lower quality with a spread in concentration of 0.005. Quite high quality of the samples as well as the temperature control up to 0.05 K allowed to obtain critical amplitudes ratios and exponents with good accuracy. However, systematic errors, which were assumed to be due to the resolution corrections, the quasi-elastic approximation, concentration fluctuations and background effects, appeared to be of more importance than statistical ones. The authors stressed that since no correction-to-scaling terms were used, the exponents found are effective ones. However the $p = 0.75$ sample was shown to exhibit RIM critical behaviour over the reduced temperature interval $4 \times 10^{-4} < |\tau| < 2 \times 10^{-1}$, whereas the critical exponents at higher dilution $p = 0.5$ had not reached their asymptotic RIM values (see Table I and figure 4).

The results mentioned above for the single crystal of transition metal fluorides were corroborated [6] by neutron scattering technique for a sample of dysprosium aluminum garnet $\text{Dy}_3\text{Al}_5\text{O}_{12}$ powder. A powder was prepared of this cubic non-collinear Ising antiferromagnet together with non-magnetic Yttrium to avoid gradients in composition which unavoidably occur. The critical exponent β increased in disordered sample in comparison to the value of the “pure” Ising model (see Table I) and provided an extra evidence of the mapping between experiment and theoretical insight.

It is known that static critical behaviour of the diluted Ising magnet in a uniform field H along the uniaxial direction behaves according to the random-field Ising model [96,97]. The random-field Ising model is the subject of intensive recent experimental studies (see [98,2] for a review). Two studies on the NS measurements in RIM appeared in the middle of 90th in the context of random-field model investigations [15,16]. In the NS studies the problem of the Bragg scattering saturation due to extinction effects was reduced by growing a $3.4 \mu\text{m}$ epitaxial film of $\text{Fe}_{0.5}\text{Zn}_{0.5}\text{F}_2$ on a (001) ZnF_2 substrate. The small X-ray rocking curve line-width of the (002) reflection showed the film to be of very high quality which was in part due to the nearly identical a -axis lattice parameters of the substrate and substance. Nevertheless, the film contained 10^4 lattice spacings and could be considered as a three-dimensional object as was proven in FeF_2 showing the critical behaviour of the “pure” $d = 3$ Ising magnet [99]. The transverse (100) Bragg scattering scans data appeared to be well described by a Gaussian distribution with a background term. Fitting the Bragg amplitude vs temperature to the simple power law a critical exponent $\beta = 0.35$ was found for $H = 0$, however, a rounding of the expected critical behaviour of the magnetization close to T_N prevented an accurate analysis of the data. To reveal whether this was caused by poor sample quality the measurements on the $3.4 \mu\text{m}$ film of $\text{Fe}_{0.52}\text{Zn}_{0.48}\text{F}_2$ were performed [16]. The higher resolution data confirmed the value of β obtained and showed that rounding was only due to resolution. Recently in a thin crystal of 0.44 mm the scattering measurements were extended from $|\tau| \geq 10^{-2}$ to $|\tau| \geq 10^{-4}$ to obtain the correlation length and susceptibility critical exponents [19,18,20].

The Mössbauer spectroscopy (MS) studies of the critical behaviour started in 1986 on a class of Fe-based substances with various magnetic atom concentrations [8]. The method was tested earlier for the “pure” Ising antiferromagnet FeF_2 , where the sublattice magnetization was shown to be proportional to the iron hyperfine field h which can be measured in MS [90]. To apply the approach to a dilute magnet, the variation of the concentration of Zn was reduced to 10^{-4} and a temperature stability of 0.002 K was achieved. In order to fix the critical temperature the values of β were chosen such that the plot $h(T)^{1/\beta}$ vs T became a straight line intercepting the abscissa axis at T_N . This method appeared to be not sensitive to particular values of β and gave the accuracy 0.05 K for critical temperature location. Though the critical exponent β can be obtained from the curve slope in double-logarithmic plot, this method produced results only after separating the data into two intervals in τ which were characterized by obviously different critical exponents: one of the “pure” Ising model and the other one of RIM. The crossover in β occurred within a very narrow range and at relatively large values of $10^{-1} \geq |\tau| \geq 10^{-3}$ for small dilution $p \geq 0.93$. The subsequent MS study appeared two years later [11] and is characterized by a very detailed analysis of the data. An advantage was the high quality of the sample grown from a stoichiometrical mixture of FeF_2 and ZnF_2 powders, each prepared by reacting a metal sponge with dry HF at $+900^\circ$. In the experiment concentration gradients in a single crystal absorber were minimized by choosing the direction of the γ -ray parallel the growth axis, both perpendicular to the plane of the sample disk of exposing sizes $4 \times 5 \times 0.1$ mm. 20 constant-acceleration spectra were obtained within $3 \times 10^{-4} < |\tau| < 0.86$. Very good temperature stability 3 mK/day and account of correction-to-scaling permitted to obtain the asymptotic RIM magnetization critical exponent β from the data in the investigated interval (see Table I).

The optical linear birefringence method (LB) introduced in Ref. [5] for the study of critical behaviour of the magnetic part of the specific heat c_m in disordered magnets was continued in Refs [13,14,19]. The proportionality between the temperature derivative $d(\Delta n)/dT$ of the optical birefringence Δn and c_m is assumed for studies of optically transparent materials. While the caloric properties in the critical region can be measured also by the pulsed heat technique, the LB method has several advantages: first of all, the non-magnetic contribution to the temperature derivative of the optical birefringence is insignificant, contrary to thermal techniques where the non-magnetic phonon background is often large and difficult to eliminate; secondly, one can minimize the concentration fluctuations effects by applying a laser beam perpendicularly to the concentration gradients. In the first experiment [13] a class of single crystals with various impurity concentration showed the exponent α to be independent of concentration and in very good agreement with the theoretical predictions (see Table III), while the two subsequent studies [19,14] showed the equivalence of

the LB method results with the direct heat pulsing measurements. Magnetic X -ray scattering successfully applied to the “pure” Ising crystal [100] was applied to the “random” Ising crystal for high dilution in Ref. [10]. For samples of sizes $5.7 \times 6.4 \times 8.9$ mm and of good crystallographic as well as mosaic quality the mean-field value for the exponent β has been found up to $|\tau| \leq 0.06$, while closer to T_N an exponent β consistent with the RIM value was obtained.

IV. MONTE CARLO SIMULATIONS

The power-law singularities like (2) in physical quantities only appear in the thermodynamic limit when the system volume and the number of particles tend to infinity. Therefore an obvious obstacles in computer “experiments” is that simulations can be done for a system of finite size only. Moreover the asymptotic temperature interval fails to be reached since T_c itself is not known exactly, whereas the location of the critical temperature is crucial for the accuracy of critical exponents determination. One can extrapolate to the thermodynamic limit assuming that the regime of a constant asymptotic critical exponent is established already starting from a certain finite system size and within an interval around T_c of a certain non-zero size. The last assumption exploited in computer simulations leads to a very narrow temperature intervals below and above T_c reliable for data sampling. The upper bounds are the temperatures where correction-to-scaling accounts for, while the lower bounds follow from finite-size effects and are of order 10^{-3} for typical system sizes achieved now in the Monte Carlo (MC) simulations. Therefore, the exponents obtained in the manner described often are effective critical exponents which characterize the critical behaviour in the observable temperature range. On the other hand different time scales govern the dynamical behaviour of pure and disordered spin systems and only very long-running simulations yield reliable data. The relaxation time increases drastically not only when approaching T_c . Moreover, in the early simulations it increased also with dilution and yielded in several decades greater values when passing from a pure $p = 1$ system to a diluted one with $p = 0.6$. However an application of a more elaborated simulation technique resulted in an opposite behaviour: the decrease of the relaxation time for a certain disordered sample with an increase of p [102]. And it is the configurational averaging that leads to overall increase of the computation time. The statistical errors for thermodynamic observables result mainly from variance in configurational space and are larger than usual statistical errors in finite-size simulations with usual now statistics of 10^6 MCS (Monte Carlo steps per spin). Consequently, the accuracy is bounded by the available CPU time from one side and limited by the number of samples to perform the configuration average of a disordered model [76] from the other side. Efficient algorithms together with high-speed computers partially solve the task.

Despite of this unpleasant situation Monte Carlo studies provided deep insight into the origin of the phase transition in the RIM as well as resulted in reliable numerical values for the critical exponents. MC studies of three dimensional RIM systems have been carried out over the last two decades [21–40]. The first search [21] for universal critical characteristics of a RIM was performed on a simple cubic lattice of a size up to 30^3 on the basis of an importance sampling MC method [101]. The positions of specific heat peaks corresponding to finite-lattice pseudo-critical temperature were extrapolated by means of finite-size scaling theory to T_c , and the accuracy of 500 – 5000 MCS per data point with averaging over several different starting configurations of impurities did not allow to discriminate between disorder relevance or irrelevance. From a fit the value of the order parameter exponent β and the susceptibility exponent γ of RIM could not be distinguished within the error bars from the corresponding exponents of the pure (non-diluted) system for any dilution (see Table II, Ref. [21]). As a possible explanation it was stated that the lattice studied were too small to reach the critical region. The predictions of the authors that “impure” critical behaviour can be observed only for systems with larger critical regions (larger α_{pure}) was objected by the MC simulations of RIM on larger lattices with narrower dilution range [22], higher statistics of $5000 \div 11000$ MCS, larger number of averaged samples and more detailed analysis of simulational data. The phase transition temperature T_c was located by adjusting data of specific-heat and numerical derivative of the energy. In this way the critical temperature accuracy was improved to 0.004 and the relevance of disorder for the universal critical properties was concluded. This result was confirmed by magnetization data, though the critical exponent β was found to vary continuously with the magnetic sites concentration and no temperature region with constant β was found. Similarly to Ref. [21] the authors of Ref. [22] stressed that while they cannot exclude the existence of a tiny impure critical region it must be unobservable for the weak dilution experimentally as well as by Monte Carlo methods, and effective critical exponents varying continuously with dilution would always show up according to the two fixed points scenario (see fig. 2). Even the possibility of the existence of a line of fixed points, one for each impurity concentration, was not excluded (compare the dependence of the magnetization critical exponent β on the concentration of magnetic sites in Table II, Ref. [22]).

The results mentioned above appeared to be in a good agreement with the MC data of Ref. [23] obtained on the basis of a multi-spin coding program where twice as large systems and 8000 MCS statistics were used for a given concentration and temperature. The effective exponent β was found to increase continuously with dilution as well. However this was believed to be a consequence of the fact that one needs to compute the equilibrium magnetization

much closer to the critical point. Two years later the conclusion that reliable critical exponent values could not be obtained by the simulation of systems with sizes $l \leq 20$ was drawn in Ref. [24]. Statistical errors in the determination of the critical temperature from susceptibility and/or specific heat data, together with the extrapolation by finite-size scaling were thought to be responsible for this situation. In particular correction-to-scaling [103] should be taken into account. Instead, the simulation with the statistics $5000 \div 11000$ MCS, but no configuration average allowed a determination of the exponent β obviously larger than the pure one, while the determination of γ were not done because of a large scatter of the data. A reanalysis of the previous MC simulations [21–23] led the authors to the conclusion that a large part of critical regime is dominated by the crossover from the pure Ising exponents to RIM ones: the results of Ref. [21] may correspond to a plateau value of the effective critical exponent governed by the pure Ising fixed point, while refined results of Refs [22,23] correspond to an intermediate regime before the asymptotic regime, unaccessible near T_c , is reached. Enforcing the concept of effective critical exponents [68,69] (see formula (2)) the authors of Ref. [24] claimed that the effective exponents they found were in qualitative agreement with the renormalization group flows (see fig. 2).

Soon it became clear that the concentration dependence of the critical exponents observed previously in MC simulations may be also due to large relaxation time at criticality. The Swendsen-Wang algorithm applied to RIM simulation of Ref. [26] resulted in the conclusion that a finite-size analysis of susceptibility data is inadequate to check the new critical exponents appearance for a RIM since the ratio γ/ν does not change with the system size. On the other hand, the determination of T_c from susceptibility maxima and the fourth-cumulant intersection method allowed to calculate the effective critical exponent γ by fitting the data points in successive time intervals. In this way the susceptibility and the correlation length critical exponents were found to be independent of concentration in a wide range of dilution (see Table II, Ref. [24]). As observed in Ref. [26] the exponent γ appeared to be higher than the theoretical asymptotic value. Thus it has been argued that γ_{eff} is a non-monotonic function of reduced temperature with a maximum value, the larger the bigger the dilution. For the particular case of magnetic sites concentration 0.8 the prediction was investigated in Ref. [27] by the Swendsen-Wang algorithm and the single-cluster generalization of Wolf for a rather large system. While the γ/ν ratio confirmed the result of Ref. [26], the effective critical exponent γ did not show a maximum but increased continuously approaching T_c .

The assumption that the interaction among block-spins in diluted systems may be represented by renormalized couplings of pure systems was used in the MC renormalization group approach for RIM in the weak dilution region ($p \geq 0.8$) [28]. The values for the correlation length critical exponent ν were found to depend on the concentrations of the magnetic sites. For $p = 0.8$ ν satisfied the exact inequality $\nu > 2/d$ for a diluted system [72] and this led the authors of Ref. [28] to the assumption that they obtained the asymptotic value of the correlation length critical exponent. They subsequently estimated the width of the asymptotic critical region for this dilution ($|\tau|_{crit} \leq 3 \cdot 10^{-4}$) where no influence of the pure Ising model fixed point is seen. Alternatively, for $p = 0.9$ the inequality [72] is not satisfied for ν and either the critical region $|\tau|_{crit} \leq 1.3 \cdot 10^{-4}$ was not reached and thus the critical behaviour is that of pure Ising model, or the crossover to the RIM asymptotical critical behaviour for $p = 0.9$ is observable only in larger systems. For $p = 0.4$ the accuracy of data obtained was too poor to find any values.

Precise MC data of Ref. [29] became available by application of the new cluster algorithm [104] and a refined vectorized implementation of local algorithms [105]. A progress in MC studies occurred when an improved version of the multi-spin coding program appeared [105,29]. It allowed to verify all previously obtained simulation data for the RIM with the unprecedented statistics of up to 3×10^5 MCS and 10 averaged configurations for systems with $p \geq 0.8$ and up to 1.2×10^6 MCS for higher dilution. For instance, in the test simulation the statistics allowed to obtain the susceptibility and magnetization critical exponents of a $2d$ pure Ising model with an accuracy of 1% and 3% respectively. For the RIM, the effective exponents γ, β and $\zeta = 1 - \beta$ (the last one describes the divergence of the magnetization-energy correlation function) were obtained [29] and were shown to be concentration dependent in the concentration region $0.5 \leq p < 1$ (see Table II). The T_c value as well as γ were obtained by fitting susceptibility data to a simple power law; the T_c location was then verified by the 4th and 6th cumulant of magnetization. The investigation of the energy-magnetization correlation function allowed to check if scaling holds; the critical exponents ζ and β were obtained by fitting the data to the simple power law with the value T_c taken from the susceptibility analysis. All data showed power-law behaviour within the chosen temperature range but the constant values of critical exponents changed with concentration (see figure 6). For instance, γ increased from the pure Ising value and smoothly changed with dilution achieving plateau value at $p = 0.5$, β similarly increases while ζ decreases in such a way that their sum equals 1 within errors. The conclusion of Ref. [29] states that while new critical exponents changing with the dilution were observed, no line of stable fixed points exists as supposed e.g. in [22]. The result originates from a crossover from pure to diluted and percolation to diluted regimes with effective exponents for all concentrations.

The evidence of crossover phenomena motivated the authors to undertake a more systematic study. The data of Ref. [29] were revised three years later in Ref. [30] where a cumulant method was used in order to determine T_c . For thermal averaging up to 40000 MCS were performed and for the configurational averaging up to 32 configurations were used (compare this with 5000 MCS and only several samples for the configurational average in Ref. [21]). The

critical exponents ζ , β and γ were shown to vary with concentration in consistency with the two fixed point scenario for the weak dilution. However for the strong dilution ($p = 0.5, 0.6$) an influence of another “percolative” fixed point was assumed. A central part of Ref. [30] dealt with the magnetization-energy scaling function. It was shown that dilute systems have a complex crossover behaviour before they reach their asymptotic critical region with values for the exponents consistent with the weak random fixed point. For instance, pure systems reach their asymptotic limit for small system size. In weakly random systems ($p \geq 0.8$) the asymptotic values for the exponents are smoothly approached from below whereas in strongly diluted systems from above. This happens at the characteristic system size λ_p depending on the concentration p . λ_p was estimated as $20 \div 30$ lattice constants for pure, 50 for $p = 0.95, 0.9$ and about $100 \div 150$ for $p = 0.6$; at the percolation point λ_p diverges. Thus more strongly disordered systems necessitate a refined analysis with an appropriate treatment of their percolative structural effects relevant for non-asymptotic sizes and correlation lengths. Accidentally the crossover function changes its sign at $p \sim 0.8$ so the asymptotic values appear to be reached already for small systems (c. f. Refs [27,29]).

Due to works [26,27] and especially [29,30] it became clear that the concentration dependent critical exponents found in MC simulations are effective ones, characterizing the approach to the asymptotic region. This point of view found its support in a conjecture about a step-like universality of the 3d diluted magnets [31]. An attempt to study the diluted model at $p = 0.6$ by means of taking MC data from different subsystems of one large system was made in Ref. [32]. It was concluded that the resulting values of the critical exponents are strongly influenced by the size of the system.

Recently, the critical behaviour of the RIM was reexamined by MC method in Refs [34,35] for concentrations $p = 0.8, 0.6$ and in Ref. [33] for $0.4 \leq p \leq 0.9$ respectively. In particular, the simulations [35] revealed that a disorder realized in a canonical manner (fixing the fraction of magnetic sites) leads to different results in comparison with disorder realized in a grand-canonical manner (see Table II). Studies of Ref. [33] were based on the importance of taking into account the leading correction-to-scaling term in the infinite volume extrapolation of the MC data and thus the analysis does not agree with the data of Ref. [35]. The results of the simulations for the concentrations $p = 0.9, 0.8, 0.6, 0.4$ were extrapolated to infinite system size (see figure 7) and lead to the proof of universal critical behaviour of the site-diluted Ising model in a wide range of concentrations. In particular the value of the correction-to-scaling exponent ω was found to be $\omega = 0.37 \pm 0.06$ which is almost half as large as the corresponding value in the pure $d = 3$ Ising model [73] $\omega = 0.799 \pm 0.011$. The smaller the value of ω the larger the interval where it has to be taken into account (c.f. formula (3) of the chapter I). Thus the smallness of ω in the dilute case explains its importance for an analysis of the asymptotic critical behaviour.

Another important question considered in Refs [34,35] is the problem of self-averaging in RIM. The Gibbs approach to the static collective phenomena rests on the statistical independence of macrosamples according to the short range nature of inter-particle interactions. In agreement with this approach any thermodynamic extensive quantity M is (strongly) self-averaged. It means that the normalized square width R_M of the squared variance of its sub-sample values behaves as $R_M = V_M/M^2 \sim 1/n \sim l^{-d}$, where n is the number of sub-samples and l is the system linear size. However, in the vicinity of the critical point the statistical independence does not hold since the correlation length of a system ξ can be arbitrary large $\xi \sim l$, and thus subsystems cannot be considered as independent. The concept of weak self-averaging takes account of the case when a number $x_1, 0 < x_1 < d$ exists such that R_M at criticality scales as l^{-x_1} . In contrary, if $R_M \rightarrow \text{const} \neq 0$, M is called to be not self-averaging. It has been predicted on the basis of heuristic arguments that for random models all extensive quantities are strong self-averaging far from criticality. Yet for a quantity M scaling at the critical point as l^ρ the strong self-averaging should fail. Here the squared variance V_M is expected to scale as $l^{2\rho+\alpha/\nu}$ for $\alpha_{random} < 0$ implying $R_M \sim l^{\alpha/\nu}$ or weak self-averaging [106].

Lack of self-averaging in RIM is not only of high theoretical interest. The reliability of MC simulations depends on the answer whether the increase of the lattice size improves the statistics of the simulations. If a quantity is not self-averaging the simulational data are unreliable. Theoretical studies based on the renormalization group approach confirmed the strong self-averaging for $l \gg \xi$. In contrast, special MC investigations in finite systems found no self-averaging in the case of relevant disorder $\alpha_{pure} > 0$, while weak self-averaging appeared to be the case only for irrelevant disorder [107], in disagreement with Ref. [106]. The MC simulations of the Refs [34,35] were performed in order to resolve this puzzle. It was shown that the normalized square width R_M goes to a constant for large l , which is *independent* from the dilution of grand-canonical type, while this is not the case for the canonical type [34]. The last result, however, may have its explanation in the very slow approach of R to its universal asymptotic value in the case of canonical realization of 3d random Ising model, estimated as $l^{\alpha/\nu}$ [36].

The evolution of the self-averaging from pure Ising model to RIM has been studied recently [37] in order to determine the transition zone between pure and diluted Ising models’ universality classes. It was shown that the transition zone is smoothly dependent on concentration of magnetic sites and independent of lattice size. In contrary, critical exponents values did not depend on concentration and were found identical to previous data of Ref. [33]. The universal value of the normalized square width of the susceptibility in the infinite-volume limit was estimated to equal $R_\chi(\infty) = 0.155$.

Apart from short-range site-dilution other realizations of disorder have become a subject for MC simulations recently.

Thermally diluted Ising model has been studied as a generalization of the RIM [38,39]. There, the realization of the vacancy distribution is determined from the local distribution of spins in a pure Ising model at criticality. The critical properties, in particular, the universality class of the model appeared to differ strongly from the RIM one, however, they agreed well with the theoretical predictions for long-range-correlated disorder [108,109].

The problem whether the RIM fixed point also describes the phase transition in the Ising model with random bonds has been studied explicitly in Refs [40,41]. Using a numerical renormalization-group analysis the RG flows for random Ising models have been obtained and the existence of a fixed point characterizing the random Ising model irrespectively to the type of disorder has been shown [40].

V. RENORMALIZATION GROUP THEORY EXPANSIONS

In the subsequent sections V and VI we will review results on RIM critical exponents obtained by means of renormalization group (RG) methods. In section V we report the main relations of the field theoretical RG approach and dwell upon perturbation expansion series available. Section VI deals with the RG series resummation methods and the results obtained on their basis.

A. Renormalization

To describe theoretically the long-distance properties arising in different systems in the vicinity of the second order phase transition point it is standard now to use a field theoretical RG approach [111,112]. The renormalization is used to remove divergences that occur during evaluation of the bare vertex functions in the asymptotic limit. For the RIM one-particle irreducible bare vertex functions are defined as:

$$\delta(q_1 + \dots + q_N)\Gamma_0^N(q_1, \dots, q_N; m_0, u_0, v_0; \Lambda_0) = \int e^{i(q_1 r_1 + \dots + q_N r_N)} \langle \varphi(r_1) \dots \varphi(r_N) \rangle_{\text{1PI}}^{\mathcal{H}_{\text{RIM}}} dr_1 \dots dr_N, \quad (12)$$

where the angular brackets denote statistical average over the Gibbs distribution with the Hamiltonian (8) in the replica limit $n \rightarrow 0$ and the subscript $_{\text{1PI}}$ indicates that only one-particle irreducible diagrams are taken into account. The functions depend on sets of momenta q_1, \dots, q_N (with Λ_0 as a momentum cutoff) and the bare parameters m_0, u_0, v_0 of the Hamiltonian (8). Divergences in (12) occur in the asymptotic limit $\Lambda_0 \rightarrow \infty$. Their removing is achieved by a controlled rearrangement of the series for the vertex functions. Several asymptotically equivalent procedures serve this purpose. For the purpose of this presentation we will use two complementary approaches: **(i)** dimensional regularization and the minimal subtraction scheme [113] and the fixed dimension renormalization at zero external momenta and non-zero mass (a massive RG scheme) [114].

Let us formulate relations of the renormalized theory. The renormalized fields, mass and couplings ϕ, m, u, v are introduced by:

$$\varphi = Z_\phi^{1/2} \phi, \quad (13)$$

$$m_0^2 = Z_{m^2} m^2, \quad (14)$$

$$u_0 = \mu^\varepsilon \frac{Z_{4,u}}{Z_\phi^2} u, \quad (15)$$

$$v_0 = \mu^\varepsilon \frac{Z_{4,v}}{Z_\phi^2} v. \quad (16)$$

Here, $\varepsilon = 4 - d$, μ is a scale parameter equal to the renormalized mass at which the massive scheme [114] is evaluated or in the minimal subtraction scheme [113] it sets the scale of the external momenta. $Z_\phi, Z_{m^2}, Z_{4,u}, Z_{4,v}$ are the renormalizing factors. The renormalized vertex functions Γ_R^N expressed in terms of the bare vertex function by:

$$\Gamma_R^N(q_1, \dots, q_N; m, u, v) = Z_\phi^{N/2} \Gamma_0^N(q_1, \dots, q_N; m_0, u_0, v_0). \quad (17)$$

are finite. This is the main content of the multiplicative renormalizability of the field theory defined by the Hamiltonian (8).

First let us consider *the minimal subtraction scheme*. Here, the renormalizing Z -factors (13)–(16) are determined by the condition that all poles at $\varepsilon = 0$ are removed from the renormalized vertex functions. The RG equations are

written bearing in mind that the bare vertex functions Γ_0^N (12) do not depend on the scale μ , and therefore their derivatives with respect to μ at fixed bare parameters are equal to zero. So one gets

$$\mu \frac{\partial}{\partial \mu} \Gamma_0^N|_0 = \mu \frac{\partial}{\partial \mu} Z_\phi^{-N/2} \Gamma_R^N|_0 = 0, \quad (18)$$

where the index $|_0$ means a differentiation at fixed bare parameters. Then the RG equation for the renormalized vertex function Γ_R^N reads:

$$\left(\mu \frac{\partial}{\partial \mu} + \beta_u \frac{\partial}{\partial u} + \beta_v \frac{\partial}{\partial v} + \gamma_m m \frac{\partial}{\partial m} - \frac{N}{2} \gamma_\phi \right) \Gamma_R^N(m, u, v, \mu) = 0, \quad (19)$$

and the RG functions are given by

$$\beta_u(u, v) = \mu \frac{\partial u}{\partial \mu} |_0, \quad (20)$$

$$\beta_v(u, v) = \mu \frac{\partial v}{\partial \mu} |_0, \quad (21)$$

$$\gamma_\phi = \mu \frac{\partial \ln Z_\phi}{\partial \mu} |_0, \quad (22)$$

$$\gamma_m(u, v) = \mu \frac{\partial \ln m}{\partial \mu} |_0 = \frac{1}{2} \mu \frac{\partial \ln Z_{m^2}^{-1}}{\partial \mu} |_0. \quad (23)$$

Using a method of characteristics [115] to solve the partial differential equation (19) one can write a formal solution as:

$$\Gamma_R^N(m, u, v, \mu) = X(\ell)^{N/2} \Gamma_R^N(Y(\ell)m, u(\ell), v(\ell), \mu(\ell)), \quad (24)$$

where the characteristics are the solutions of the ordinary differential equations (flow equations):

$$\begin{aligned} \ell \frac{d}{d\ell} \ln X(\ell) &= \gamma_\phi(u(\ell), v(\ell)), & \ell \frac{d}{d\ell} \ln Y(\ell) &= \gamma_m(u(\ell), v(\ell)), \\ \ell \frac{d}{d\ell} u(\ell) &= \beta_u(u(\ell), v(\ell)), & \ell \frac{d}{d\ell} v(\ell) &= \beta_v(u(\ell), v(\ell)) \end{aligned} \quad (25)$$

with

$$X(1) = Y(1) = 1, \quad u(1) = u, \quad v(1) = v. \quad (26)$$

For small values of ℓ , equation (24) maps the large length scales (the critical region) to the non-critical point $\ell = 1$. In this limit the scale-dependent values of the couplings $u(\ell)$, $v(\ell)$ will approach the stable fixed point, provided such a fixed point exists. The fixed points u^* , v^* of the differential equations (25) are given by the solutions of the system of equations:

$$\begin{aligned} \beta_u(u^*, v^*) &= 0, \\ \beta_v(u^*, v^*) &= 0. \end{aligned} \quad (27)$$

The stable fixed point is defined as the fixed point where the stability matrix

$$B_{ij} = \frac{\partial \beta_{u_i}}{\partial u_j}, \quad u_i = \{u, v\} \quad (28)$$

possesses eigenvalues ω_1, ω_2 with positive real parts. The stable fixed point, which is reached starting from the initial values ℓ_0 in the limit $\ell \rightarrow 0$, corresponds to the critical point of the system. In the limit $\ell \rightarrow 0$ (corresponding to the limit of an infinite correlation length) the renormalized couplings reach their fixed point values and the critical exponents η and ν are then given by

$$\eta = \gamma_\phi(u^*, v^*), \quad (29)$$

$$1/\nu = 2(1 - \gamma_m(u^*, v^*)). \quad (30)$$

In the non-asymptotic region but near the fixed point deviations from the power laws with the fixed point values of the critical exponents are governed by the correction-to-scaling exponent

$$\omega = \min(\omega_1, \omega_2) \quad (31)$$

in accordance with the Wegner expansion [70] (3). The rest of the critical exponents are obtained by familiar scaling laws [67,111]:

$$\alpha = 2 - d\nu, \quad \beta = \frac{\nu}{2}(d - 2 + \eta), \quad \gamma = \nu(2 - \eta) \quad (32)$$

which can be shown to hold from the solutions (24).

The flow equations (25) can serve to describe the approach to criticality in a larger region where corrections to scaling do not suffice. As it was mentioned in chapter I out of the asymptotic region physical observables are characterized by effective exponents introduced to describe a crossover from the background behaviour to the asymptotic critical one. In the RG language they depend on the flow parameter $\ell(\tau)$ through the dependence of couplings on ℓ . In particular, according to the definition (see formula (2)) for the magnetic susceptibility effective exponent γ_{eff} we have:

$$\gamma_{eff}(\tau) = \frac{d \ln \chi(\tau)}{d \ln \tau} = \gamma(u(\ell(\tau)), v(\ell(\tau))) + \dots, \quad (33)$$

where the second part is proportional to the β -functions and comes from the change of the amplitude part of the susceptibility. This part is natural to neglect in the vicinity of a fixed point. Moreover, the contribution of the amplitude function to the crossover does seem to be small [116,117]. Under this restriction, the effective exponents are simply given by the expressions for the asymptotic exponents (30) but with replacing the fixed point values of the couplings u^*, v^* by the solutions of the flow equations (25):

$$\begin{aligned} \eta_{eff}(\ell) &= \gamma_\phi(u(\ell), v(\ell)), \\ 1/\nu_{eff}(\ell) &= 2(1 - \gamma_m(u(\ell), v(\ell))). \end{aligned} \quad (34)$$

In the *massive RG scheme* the Z -factors (13)–(16) are calculated from the vertex functions (12) at zero external momenta q_1, \dots, q_N and non-zero mass at fixed space dimension in the limit $\Lambda_0 \rightarrow \infty$. This normalization conditions lead to the equation for the renormalized vertex functions which is called Callan–Symanzik equation. Differentiation of the proper bare vertex function Γ_0^N with respect to the renormalized mass (c.f. eq. (18)) gives:

$$m \frac{\partial}{\partial m} \Gamma_0^N |_0 = m \frac{\partial m_0^2}{\partial m} |_0 \Gamma_0^{(1,N)}, \quad (35)$$

again, the index $|_0$ means a differentiation at fixed bare parameters and a new vertex function

$$\Gamma_0^{(1,N)} = \frac{\partial \Gamma_0^N}{\partial m_0^2} \quad (36)$$

appears. This vertex function differs from Γ_0^N by an extra term $\phi^2(R)$ inside the averaging $\langle \dots \rangle$ in (12). As a result, for the renormalized vertex functions Γ_R^N one gets an inhomogeneous Callan–Symanzik equation containing $\Gamma_R^{(1,N)}$ in the right-hand side. However, close to the critical point $m = 0$ the right-hand side can be neglected with respect to the left-hand side and one arrives to the homogeneous Callan–Symanzik equation which repeats the structure of the RG equation (19):

$$\left(m \frac{\partial}{\partial m} + \beta_u \frac{\partial}{\partial u} + \beta_v \frac{\partial}{\partial v} - \frac{N}{2} \gamma_\phi \right) \Gamma_R^N(m, u, v) = 0, \quad (37)$$

where the coefficients $\beta_u, \beta_v, \gamma_\phi$ are defined by the relations (20)–(22), but the parameter μ there is to be understood as the renormalized mass m . The partial differential equation (37) is solved again by the characteristics method sketched by the relations (24)–(26) and leads to the fixed point relations given by (27)–(31).

For the sake of completeness let us note that the finiteness of the renormalized vertex function with one ϕ^2 insertion $\Gamma_R^{(1,2)}$ is achieved by the familiar renormalizing factor \bar{Z}_{ϕ^2} :

$$\Gamma_R^{(1,2)}(k; q, -q; m, u, v) = \bar{Z}_{\phi^2} \Gamma_0^{(1,2)}(k, q, -q, m_0, u_0, v_0). \quad (38)$$

Then, formula (30) for the correlation length critical exponent ν may be recast in terms of \bar{Z}_{ϕ^2} by a substitution $2\gamma_m = \gamma_\phi + \bar{\gamma}_{\phi^2}$, which follows from the relations $Z_{m^2} = \bar{Z}_{\phi^2} Z_\phi^{-1}$ and $\bar{\gamma}_{\phi^2} = \mu \partial \ln \bar{Z}_{\phi^2}^{-1} / \partial \mu|_0$. This leads to the relation:

$$1/\nu = 2 - \gamma_\phi(u^*, v^*) - \bar{\gamma}_{\phi^2}(u^*, v^*). \quad (39)$$

The explicit expressions for the RG β - and γ - functions are scheme dependent: they do differ in different renormalization schemes. Subsequently the fixed point coordinates are scheme dependent as well. However, the RG functions coincide in different schemes once calculated at the fixed point. This leads to the same asymptotic values of the critical exponents: they are universal and do not depend on renormalization scheme [111,112]. In the next subsection we will provide available expansions for the RG functions of the RIM.

B. Perturbation expansion series and their “naive” analysis

Expressions for the RG functions of the RIM are obtained as series in the renormalized couplings u and v . The perturbation theory in powers of u , v is in fact a perturbation theory in number of integrations in k -space which, on the other side, corresponds to the number of loops in Feynman diagrams in the diagrammatic representation for the vertex functions [111]. By now, the RIM RG functions are known up to the order of 5 loops in the minimal subtraction scheme [118] and with record 6 loop accuracy when calculated directly for $d = 3$ in the massive scheme [66].

Written in the minimal subtraction scheme the functions read:

$$\beta_u = -u \left(\varepsilon - u - 3/2 v + 17/27 u^2 + 23/12 uv + 41/32 v^2 + \dots + \beta_u^{(5LA)} \right), \quad (40)$$

$$\beta_v = -v \left(\varepsilon - v - 2/3 u + 21/32 v^2 + 11/12 vu + 5/27 u^2, \quad (41)$$

$$\gamma_\phi = 1/54 u^2 + 1/24 uv + 1/64 v^2 + \dots + \gamma_\phi^{(5LA)}, \quad (42)$$

$$\bar{\gamma}_{\phi^2} = 1/3 u + 1/4 v - 1/9 u^2 - 1/4 uv - 3/32 v^2 + \dots + \bar{\gamma}_{\phi^2}^{(5LA)}. \quad (43)$$

Here, we write down the functions only up to the two-loop approximation (2LA), referring to the paper [57] where they were obtained in 3LA. Four- and five-loop contributions may be derived from the RG functions of the anisotropic cubic model obtained in Ref. [118].

Note, that in the minimal subtraction scheme the dependence on the space dimension d is trivial and enters expressions (40)–(43) only via one single term proportional to $\varepsilon = 4 - d$ explicitly written in the β -functions (40), (41). On contrary, in the massive scheme the space dimension d enters the expressions for the loop integrals, corresponding to each Feynman diagram of perturbation expansion. Subsequently the theory is evaluated at space dimension of interest [121]. The series for RG functions of the $d = 3$ RIM read:

$$\beta_u = -u \left(1 - u - 3/2 v + 308/729 u^2 + 104/81 uv + 185/216 v^2 + \dots + \beta_u^{(6LA)} \right), \quad (44)$$

$$\beta_v = -v \left(1 - v - 2/3 u + 95/216 v^2 + 50/81 vu + 92/792 u^2 + \dots + \beta_v^{(6LA)} \right), \quad (45)$$

$$\gamma_\phi = 8/729 u^2 + 2/81 uv + 1/108 v^2 + \dots + \gamma_\phi^{(6LA)}, \quad (46)$$

$$\bar{\gamma}_{\phi^2} = 1/3 u + 1/4 v - 2/27 u^2 - 1/6 uv - 1/16 v^2 + \dots + \bar{\gamma}_{\phi^2}^{(6LA)}. \quad (47)$$

Again, we display here only the two-loop functions. In the ε expansion these functions were first obtained in Ref. [45]. Three-loop terms first reported in Ref. [48] contained some errors, partially corrected in Ref. [49]. Finally free of errors three-loop expressions were reported in Ref. [53]. Subsequently four-loop series were obtained in Ref. [54] and only recently five-loop [64] and record six-loop [66] expansions became available. Universal critical amplitude ratios at $d = 3$ were first obtained in three-loop approximation [119] and are known by now within the accuracy of five loops [120].

As we noted above, the massive RG scheme does not necessarily mean evaluation at $d = 3$. A possibility to apply the scheme in order to get the RIM RG functions at arbitrary non-integer space dimension was outlined in Ref. [56]. For the two-loop RG functions one gets [56]:

$$\beta_u(u, v) = -(4-d)u \left\{ 1 - u - \frac{3}{2}v + \frac{8}{27} \left[9(i_1 - \frac{1}{2}) + i_2 \right] u^2 + \frac{2}{3} \left[12(i_1 - \frac{1}{2}) + i_2 \right] uv + \frac{1}{4} \left[21(i_1 - \frac{1}{2}) + i_2 \right] v^2 \right\}, \quad (48)$$

$$\beta_v(u, v) = -(4-d)v \left\{ 1 - v - \frac{2}{3}u + \frac{1}{4} \left[11(i_1 - \frac{1}{2}) + i_2 \right] v^2 + \frac{2}{3} \left[6(i_1 - \frac{1}{2}) + i_2 \right] vu + \frac{8}{27} \left[3(i_1 - \frac{1}{2}) + i_2 \right] u^2 \right\},$$

$$\begin{aligned}\gamma_\phi(u, v) &= -2(4-d) \left\{ \left[\frac{2}{27}u^2 + \frac{1}{6}uv + \frac{1}{16}v^2 \right] i_2 \right\}, \\ \bar{\gamma}_{\phi^2}(u, v) &= (4-d) \left\{ \frac{1}{3}u + \frac{1}{4}v - 12 \left[\frac{1}{27}u^2 + \frac{1}{12}uv + \frac{1}{32}v^2 \right] \left(i_1 - \frac{1}{2} \right) \right\}.\end{aligned}\tag{49}$$

The space dimension d enters expressions (48)–(50) also by the d -dependent two-loop integrals $i_1(d)$, $i_2(d)$. Their dependence on d is shown in the figure 8. Evaluating the integrals [121] for $d = 3$: $i_1(3) = 2/3$, $i_2(3) = -2/27$ one recovers the two-loop contributions of the expressions (44)–(47). In next order of perturbation theory for non-integer d the RIM was derived in Ref. [60], the values of the corresponding loop integrals are obtained in Ref. [122].

With the series for the RG functions at hand there are two different ways to proceed in any of the two RG approaches (40)–(43) or (44)–(47). Subsequently, this leads to four different schemes for our analysis. Indeed, the minimal subtraction scheme can be realized by the familiar ε -expansion [123] as well as directly at $d = 3$ [124]. Similarly, the expressions for the RG functions obtained in the massive scheme can be directly solved for the fixed points (FP) or by the pseudo- ε expansion [125]. However, as we will see below, only two of these schemes lead to reliable results for the RIM critical behaviour. Before we proceed let us discuss this situation in more details.

- **1.** First let us consider the functions (40)–(43) and perform the ε -expansion. In order to obtain the expansion, one should (i) solve the fixed point equations (27) with ε as a small parameter and then (ii) substitute the coordinates $u^*(\varepsilon)$, $v^*(\varepsilon)$ as series in ε into the RG- γ -function for the critical exponents for critical exponents.

Looking for the fixed point solutions in one-loop approximation (i.e. leaving only linear in u, v terms in the brackets in (40), (41)) one finds three fixed point (compare with the fig. 2): the Gaussian fixed point **G** $u^* = v^* = 0$, the pure Ising fixed point **I** $u^* \neq 0$, $v^* = 0$ (it describes n non-interacting Ising models: c.f. Hamiltonian (8) with $v = 0$) and the “polymer” fixed point **P** $u^* = 0$, $v^* \neq 0$ (putting $u^* = 0$ in (8) one gets the $O(n = 0)$ -model describing the scaling properties of self-avoiding walks). It is straightforward to check that the fixed points **G** and **I** are unstable whereas the fixed point **P** is stable but as far as $v^* > 0$ it is inaccessible for the initial values of couplings of our model. One does not encounter in 1LA the fixed point **R** with both non-zero coordinates $u^* \neq 0$, $v^* \neq 0$: this is because the system of equations for the fixed points is degenerate on the one-loop level [42,44,45]. This fixed point appears in the next, two-loop approximation and leads to the qualitative picture shown in the figure 2. However, the degeneracy of the one-loop equations leads to the result, that instead of expanding in ε one has to expand in $\sqrt{\varepsilon}$ [43,45]. Proceeding as usual this leads to a $\sqrt{\varepsilon}$ expansions for the critical exponents and the stability matrix (28) eigenvalues [58,61]:

$$\nu = 0.5 + 0.08411582\varepsilon^{1/2} - 0.01663203\varepsilon + 0.04775351\varepsilon^{3/2} + 0.27258431\varepsilon^2,\tag{50}$$

$$\eta = -0.00943396\varepsilon + 0.03494350\varepsilon^{3/2} - 0.04486498\varepsilon^2 + 0.02157321\varepsilon^{5/2},\tag{51}$$

$$\gamma = 1 + 0.16823164\varepsilon^{1/2} - 0.02854708\varepsilon + 0.07882881\varepsilon^{3/2} + 0.56450490\varepsilon^2,\tag{52}$$

$$\omega_1 = 2\varepsilon + 3.704011194\varepsilon^{3/2} + 11.30873837\varepsilon^2,\tag{53}$$

$$\omega_2 = 0.6729265850\varepsilon^{1/2} - 1.925509085\varepsilon - 0.5725251806\varepsilon^{3/2} - 13.93125952\varepsilon^2.\tag{54}$$

Two-loop expressions for the exponents were obtained in Ref. [45], three-loop results were presented independently in Refs [46] and [47]. The $\sqrt{\varepsilon}$ -expansion series for the RIM amplitudes ratios [127] is also available in the three-loop accuracy [128]. Due to the five-loop results for an anisotropic cubic model [118] it was possible to obtain four- and five-loop $\sqrt{\varepsilon}$ -expansion for the critical exponents [58] (50)–(52) and the stability matrix eigenvalues [61] (53)–(54) of the RIM.

- **2.** The second way of calculation which may be used in the minimal subtraction RG approach is the $d = 3$ technique [124]. It consists in (i) fixing the value of $\varepsilon = 1$ in (40), (41), (ii) solving the system of fixed point equations (27) numerically and (iii) substituting the numerical values of the fixed point coordinates into the series for the critical exponents. The RIM β -functions are shown in figure 9 in two-loop approximation. One can see that they do not possess non-trivial fixed points at all! However, such behaviour is not surprising and is not a particular feature of the RIM. It is well known that perturbation series for the RG functions in the weak coupling limit are asymptotic at best and should be evaluated by means of special resummation technique. This will be the subject of the next Section VI, and here, to complete the list of possible calculation schemes we mention two more schemes in the massive RG approach:

- **3.** The massive RG scheme is implemented by (i) solving the system of fixed point equations (27) numerically and then (ii) substituting the fixed point coordinates numerical values into the series for the critical exponents. This is the way which most of the papers are devoted to in the RIM RG analysis (see the next section for more details).

- **4.** The massive RG scheme implemented by a pseudo- ε expansion [125]. This scheme is based on the observation that in order to analyze the series (44)–(47) one can imitate an ε -expansion introducing an auxiliary parameter τ instead of the zeroth-order term 1 in the massive scheme β -functions (44), (45). Then FPs and critical exponents are obtained as series in τ with substitution $\tau = 1$ to obtain their final values. The described pseudo- ε expansion

[125] allows to avoid cumulation of the errors for the critical exponents from the errors of the fixed point coordinates and the γ -functions. It proved to be highly efficient for the pure $d = 3$ Ising model [126,74]. For the same reasons as the ε -expansion for RIM turns to the $\sqrt{\varepsilon}$ expansion, the expansion in τ turns to a $\sqrt{\tau}$ -expansion. On the basis of the six-loop expansions (44)–(47) we get the following $\sqrt{\tau}$ -expansion for the RIM critical exponents and the stability matrix eigenvalues:

$$\nu = 0.5 + 0.10291260 \tau^{1/2} + 0.01251853 \tau + 0.01270178 \tau^{3/2} + 0.05663757 \tau^2 + 0.03694322 \tau^{5/2}, \quad (55)$$

$$\eta = -0.00836820 \tau + 0.02173733 \tau^{3/2} - 0.01487714 \tau^2 + 0.01733771 \tau^{5/2}, \quad (56)$$

$$\gamma = 1 + 0.20582521 \tau^{1/2} + 0.02922117 \tau + 0.01539608 \tau^{3/2} + 0.11858141 \tau^2 + 0.06658280 \tau^{5/2}, \quad (57)$$

$$\omega_1 = 2\tau + 2.59761132 \tau^{3/2} + 7.51800557 \tau^2 + 39.86825804 \tau^{5/2}, \quad (58)$$

$$\omega_2 = 0.82330084 \tau^{1/2} - 1.74713206 \tau - 1.26569350 \tau^{3/2} - 8.75074159 \tau^2 - 40.98838378 \tau^{5/2}.$$

These expressions are to be compared with the formulas (50)–(54).

VI. SERIES RESUMMATION AND NUMERICAL RESULTS

A. Summability of RIM divergent series

The core of the perturbation approach described above is the account of higher perturbation contributions. However, such a way does not lead necessarily to cumulation of the calculation accuracy by a “naive” summation of successive perturbation theory terms. It is well known by now that the weak coupling expansion series for RG functions have zero radii of convergence and are asymptotic at best [112]. Appropriate resummation procedures are to be applied in order to handle them. Early studies of critical phenomena by the ε -expansion technique lead to a concept of a series “optimal truncation” as a maximal number of terms possessing convergent behaviour. Such behaviour is typical for asymptotic series [130] where series expansion coefficients grow factorially. For example, the expansion of a RG function $f(u)$ of pure Ising model in powers of a (single) renormalized coupling u :

$$f(u) = \sum_k A_k u^k \quad (59)$$

was shown to possess the following behaviour

$$A_k = ck^{b_0} (-a)^k k! [1 + O(1/k)], \quad k \rightarrow \infty \quad (60)$$

with known values [132–134] of constants c , b_0 , a . The property (60) indicates the Borel summability of the series (59). The Borel resummation procedure takes into account the asymptotic behaviour of the coefficients (60) and maps the asymptotic series (59) to a convergent one with the same asymptotic limit. We will describe the procedure in more details in subsections VIB and VIC.

It is worthwhile to note, that there does not exist a proof of Borel-summability for the ε -expansion of a pure Ising model. Only expansion in coupling (59) is proved to possess this property [131]. Nonetheless the rich amount of numerical estimates obtained on the basis of resummed ε -expansion for the pure Ising model (see e.g. [112]) convinces one in its reliability. However it is not the case for the $\sqrt{\varepsilon}$ -expansion of RIM. The fact that ε -expansion will not be able to give information on critical exponents in system with quenched disorder was predicted already in Refs [135,136] by studying the randomly diluted model in zero dimensions. The perturbation theory series of this toy-model appeared to be Borel non-summable. Moreover, such properties were shown [136] to be the direct consequence of the existence of Griffiths-like singularities [80] caused by zeroes of the partition function of the pure system. Although the $\sqrt{\varepsilon}$ -expansion allowed to predict qualitatively new critical behaviour of the RIM [43,45] it seems to be of no use for a quantitative analysis. Moreover, from naively adding the successive perturbational contributions in the $\sqrt{\varepsilon}$ -expansion for the RIM stability matrix eigenvalues (53), (54) one observes that already in the three-loop approximation ($\sim \varepsilon$) ω_2 becomes negative and therefore no stable fixed point exists in strict $\sqrt{\varepsilon}$ -expansion [61]! Even the resummation procedures applied do not change this picture [63]. Quite different convergence properties of the expansions for pure $d = 3$ Ising model and RIM may be seen already applying simple Padé analysis as it was shown in Refs [59,63].

The above mentioned divergent properties of the $\sqrt{\varepsilon}$ -expansion concern also the pseudo- $\sqrt{\varepsilon}$ expansion (55)–(58) derived in Section V. So there remain only two out of four different ways of numerical analysis of the RIM RG functions. They are denoted by **• 2** and **• 3** in the preceding subsection VB. Both are based on analysis of RG series in two couplings. The nature of the RIM RG functions series in couplings u , v remains opened. Nonetheless, the

resummation procedures which in different modifications are used in analysis of asymptotic series have been applied fruitfully to the RIM RG series as well [51–57,59–64]. The method which prevails in the resummation of the RIM RG series is the generalization of a Padé-Borel resummation technique [137] for the case of two variables. We will review results based on such resummation in the next subsection VI B.

Recently, it was shown that the expansions for the quenched diluted Ising model in $d = 0$ dimensions are Borel summable, provided a specific way of summation is applied [138]. This allowed authors of Ref. [65] both to recover the asymptotic behaviour of expansion coefficient as well as to apply to RIM six-loop massive RG functions [66] the resummation technique refined by a conformal mapping. This method will be reviewed in the last subsection VI C.

B. Padé-Borel oriented resummation

In order to perform the Padé-Borel resummation of a truncated (asymptotic) series in a single variable (e. g. series (59) with L terms available) one defines the Borel-Leroy image of the initial sum $S = \sum_{i=0}^L a_i u^i$ by:

$$S^B(u) = \sum_{i=0}^L \frac{a_i u^i}{\Gamma(i+q+1)}, \quad (61)$$

where $\Gamma(x)$ is the Euler's gamma function and q is an arbitrary non-negative number, which will serve as a fit parameter. The result (61) is extrapolated by means of a rational approximant $[M/N](u)$, which is the quotient of two polynomials in u with M as the order of the numerator and N as that of the denominator (a Padé approximant [139]). Subsequently, the resummed function S^{res} is obtained in the form:

$$S^{\text{res}}(u) = \int_0^\infty dt \exp(-t) t^q [M/N](ut). \quad (62)$$

In the single-variable RG functions analysis this procedure was initiated in Refs [137].

There are different ways to generalize single variable Padé approximants for the case of two variables (u, v) [139] and, subsequently to generalize the resummation procedure (61), (62). One possibility is to construct the series in a single dummy variable x (so-called resolvent series [140]). The variable is introduced by a substitution $u \rightarrow ux$, $v \rightarrow vx$ and x must be put equal to 1 to obtain final results. In accordance, the Borel-Leroy image of a truncated series $S = \sum_{0 \leq i+j \leq L} a_{i,j} u^i v^j$ is defined by:

$$S^B(x) = \sum_{0 \leq i+j \leq L} \frac{a_{i,j} (ux)^i (vx)^j}{\Gamma(i+j+q+1)}. \quad (63)$$

Then the series in x is resummed by formula (62) and evaluated at $x = 1$. We will refer to this method as to the Padé-Borel method similarly to the one-coupling case.

Another way to proceed is to make use of the Chisholm approximants [141,139] which are the generalization of Padé-approximants to many-variable case. A Chisholm approximant can be defined as a ratio of two polynomials both in variables u and v , of degree M and N such that the first terms of its expansion are equal to those of the function which is approximated. Again, the resummation is performed by (62) with Chisholm approximant instead the Padé one. This method will be referred below as the Chisholm-Borel resummation.

For a given Borel-Leroy image many approximants, both Padé and Chisholm, can be constructed. However, restrictions are imposed naturally. Firstly, an approximant should be chosen in the form re-constituting the sign-alternating high-order behaviour of the general term of β - and γ -functions [66]. The approximant generating a sign-alternating series might be chosen in a form $[M/1]$ with the positive coefficients at the variable x (or u and v). However, these are the diagonal approximants which give the best convergence in Padé analysis [139] (see also [63] for a toy model example). On the other hand, high degree of a polynomial in the denominator often leads to poles on the positive semi-axis. One can use analytic continuation and calculate the principal value of the integral (62) to process the singularities however practical calculations reject the generalization [137]. The reason is both unexpected shift of fixed point location and different topological structure of the lines of zeros for the resummed β -functions. The choice of a Chisholm approximant is even more complicated since often its coefficients are undetermined. For instance, already two-variable polynomials of a second order require two additional conditions to be imposed. Normally they are chosen to preserve certain symmetry properties. Provided the couplings u_0 and v_0 enter the Hamiltonian (8) symmetrically, the approximants must be symmetric in variables u and v in order not to introduce an additional symmetry. Another point is that by substitution $v = 0$ all the equations which describe the critical behaviour of the diluted model

are converted into appropriate equations of the pure model. However, if pure model is solved independently, the resummation technique with the application of Padé approximant is used. Thus, Chisholm approximant is to be chosen in such a way that, by putting any of u or v equal to zero, one reproduces familiar results for the one-variable case. This also implies a special choice of additional conditions.

Most numerical results on the universal characteristics of RIM at criticality were obtained on the basis of the massive renormalization scheme by numerically solving fixed point equations (27) for the resummed β -functions (44), (45) and resumming the γ -functions (46),(47) in the stable fixed point (scheme \bullet **3** in the subsection V B). The study of the massive β -functions of RIM resummed in this way revealed that starting from the two-loop approximation the random fixed point (**R**: see figure 2) is stable and is present in all orders of perturbation theory [51–56,60,62,64,142]. As an example, in figures 10, 11 we show the lines of zeros of functions $\beta_u(u, v)$ $\beta_v(u, v)$ in different orders of perturbation theory without resummation and resummed by the Chisholm-Borel method. One can see that without resummation all non-trivial fixed points are obtained only in the three-loop approximation. Resummation restores presence of non-trivial fixed points.

The massive scheme of field-theoretical renormalization group was the basis of first numerical estimates of RIM critical exponents. Alternatively, the non-perturbative scaling-field approach for solution of the Wilson’s renormalization-group equation was used to study RIM critical behaviour in Ref. [50]. The approach similarly to ε -expansion permits to treat model in continuous dimensions d . As a result, RIM critical exponents were found for d , $2.8 \leq d \leq 4$. However, the scaling-field approach was not followed by more precise calculations and Ref. [50] remains the only theoretical study where RIM critical exponents were obtained not on the basis of field-theoretic RG.

Already the study of two-loop RIM massive RG functions resummed by the Chisholm-Borel procedure [51] revealed that no difficulties connected to the degeneracy of the β -functions are encountered. Critical exponents extracted from resummed γ -functions values in the fixed point were found clearly larger than the pure model ones (see table III). As noted above, in the three-loop level the straightforward analysis of the β -functions [48,49] yielded fixed point coordinates and critical exponents without resummation, but the obtained accuracy did not allow to estimate, for instance, heat capacity critical behaviour. On the other hand, the application of the Padé-Borel technique also encountered hardships within the three-loop level (see diagram in the Fig. 16). Here, the approximant with linear denominator does not yield a fixed point, while another near-diagonal approximant [1/2] is unreliable because reveals fixed point only when processing the pole on the real axis via analytic continuation. The same expressions when treated by means of a Chisholm-Borel technique allowed to obtain asymptotic critical exponents [52,53].

The four-loop results [54] were resummed both by means of Chisholm-Borel [54], the first confluent form of the ϵ -algorithm of Wynn [55] and Padé-Borel [55,62] methods and showed close results (see table III as well as diagram 16). Whereas Padé-Borel calculations of Ref. [55] exploited the [3/1] Padé approximant, Ref. [62] used a more elaborated generalized Padé-Borel-Leroy resummation method. The last is based on exploiting all possible Padé approximants in the Borel-Leroy resummation (61)–(62) choosing for each of them the optimal value of the Leroy parameter q and then averaging the result over all values given by the approximants [62].

The expressions in the five-loop approximation analyzed with the application of the fit parameter q required rather artificial rejecting of many approximants [64]. For instance, using a criterion that those approximants are working, which provide maximal stability against variation of q , the approximant [2/2] was chosen to estimate u^* and the approximant [3/1] to obtain v^* . The analysis allowed the authors of Refs [64] to obtain the five-loop estimates for the RIM critical exponents (see table III). However, the extend to the six-loop order revealed a wide gap between five- and six-loop fixed point coordinates [142] with subsequent inconsistency of the six-loop values of critical exponents compared with the five-loop results of Refs [64]. This might serve as an indirect evidence of a possible non-asymptotic nature of the series under consideration.

Similar resummation technique was also applied to the minimal subtraction RG functions (40)–(43) directly at $d = 3$ (scheme \bullet **2** in the subsection V B) [57,59,61,63]. Here, asymptotic as well as effective critical behaviour was studied. Again, as in the massive RG case, resummation restores the presence of non-trivial fixed point in the two-loop approximation (see figure 12) and preserves it in three [57] and four loops [59,63]. However, in the five-loop order the applied Chisholm-Borel resummation scheme did not lead to a real root for the random fixed point [59,63]. One of reasons for such behaviour may be (possible) Borel-non-summability of the series under consideration. In this case the four-loop approximation will be an “optimal truncation” for the resummed minimal subtraction perturbation theory series, similar to the non-resummed asymptotic series, e.g. in the ε -expansion of $O(n)$ -symmetric ϕ^4 model, where “naive” interpretation of the series truncated by ε^2 term leads to the best (optimal) result.

Obtained in three- [57] and four- [59,61,63] loop approximation values of asymptotic critical exponents are listed in the table III, effective exponents were calculated [57,63] by resummation of formulas (34), (39). Figure 13 shows the solutions $u(l)$, $v(l)$ of the flow equations (25) calculated by Chisholm-Borel resummation of four-loop β -functions (40), (41) [63]. The flows shown in figure 13 allow for several different scenarios for the values of the effective critical exponents (see figs. 14, 15). Both in experiment as well as in computer simulations (see Tabs. I, II) exponents reported differ and even exceed the known asymptotic theoretical values. This non-universal behaviour might be related to the

possible non-asymptotic behaviour found in different flows as has been suggested in Refs [30,57]. The difference might be due to (i) the different temperature regions of the experiment and/or (ii) the different concentrations. The initial values for the couplings in the flow equations depend on the value of the concentration, especially for small dilution one expects the coupling v to be proportional to the concentration. If this is the case one expects a monotonous increase of the values of the effective exponent to the asymptotic value. A typical scenario is seen in curve 3 of Figs. 13, 14, 15. In this case effective exponents equal to the pure model critical exponents might be found in relatively wide region of temperature. Then as the attraction region of the fixed point \mathbf{I} becomes weaker and weaker, an overshooting is possible and effective exponents larger their asymptotic values might be found. This scenario is predicted for larger dilutions and represented by the curve 6 of Figs. 13, 14, 15. Curves 5, 6 correspond to situation when crossover from the mean field behaviour towards the random one is not influenced by the presence of a pure fixed point \mathbf{I} .

C. Resummation based on the conformal mapping

The resummation procedure based on conformal mapping is widely used in the analysis of asymptotic series for models with one coupling, in particular for the pure $d = 3$ Ising model (scalar ϕ^4 theory, see e.g. [126,74,112]). But it assumes that the behaviour of high order terms of the series expansion is known. It is not the case for the RIM and hence the Padé-Borel based resummation technique was used there as described in the former subsection VI B. However, recently by studying the $d = 0$ dimensional quenched diluted Ising model it was shown analytically [138] that the perturbative expansions for the free energy are Borel summable provided the summation is carried in a special way. The main results of Ref. [138] state that if the double expansion of the RIM functions in powers of u , v is written as

$$f(u, v) = \sum_{i=0}^{\infty} c_i(v) u^i, \quad (64)$$

$$c_i(v) = \sum_{j=0}^{\infty} c_{ij} v^j, \quad (65)$$

then the expansion (65) as well as expansion (64) at v fixed are Borel summable. These results enabled authors of Ref. [65] to perform the resummation of the six-loop series (44)–(47) [66]. Moreover, by noticing that the large order behaviour of the series (65) can be derived on the basis of known asymptotics (60) [132–134] they were able to perform the resummation based on conformal mapping for the series in v (65) to get convergent results for the coefficients $c_i(v)$.

The procedure of conformal mapping resummation of a single-variable u series is standard [126,143]. For a given Borel-Leroy transform $S^B(u)$ (61) the initial series may be regained from

$$S^{\text{res}}(u) = \int_0^{\infty} dt t^b e^{-t} S^B(ut). \quad (66)$$

Assuming the behaviour of the high order terms (60) one concludes that the singularity of the transformed series $S^B(u)$ closest to the origin is located at the point $(-1/a)$. Conformally mapping the u plane onto a disk of radius 1 while leaving the origin invariant (see figure 17),

$$w = \frac{(1 + au)^{1/2} - 1}{(1 + au)^{1/2} + 1}, \quad u = \frac{4}{a} \frac{w}{(1 - w)^2}, \quad (67)$$

substituting this into $S^B(u)$, and re-expanding in w , one receives a series defined on the disk with radius 1 in the w plane. This series is then re-substituted into Eq. (66). In order to weaken a possible singularity in the w -plane the corresponding expression is multiplied by $(1 - w)^\rho$ and thus one more parameter ρ is introduced [143].

However, the above procedure may be applied only to the RIM RG series for the coefficients c_i (65), as far as the large order behaviour (60) may be derived only for series in v (65) [65]. Asymptotics of the resulting series in u (64) is still unknown which causes an application of the Padé-Borel resummation technique for their analysis. The last can be applied to the series (65) as well. In summary this leads to different ways of series resummation: i) applying Padé-Borel method both for series (64) and (65) (in Ref. [65] this way is called a “double Padé-Borel method”) and ii) applying the conformal method for series (65) and the Padé-Borel method for series (64) (“conformal Padé-Borel method”). Both ways were implemented in Ref. [65] taking special attention to the choice of different Padé approximants as well as optimizing the results on the basis of fit parameters. In the table III we display the data for the RIM critical

exponents given by the authors on the basis of the analysis of the six-loop RG functions in such a way that both estimates obtained by the double Padé-Borel method and the conformal Padé-Borel method are included (we denote them as PdBr-CM). Separately we give the results of the analysis by the double Padé-Borel method (PdBr-PdBr). Let us note here, that the conformal mapping technique appears to give more robust results even resumming the RG series for fixed v^*/u^* . Applying a procedure of conformal-mapping based resummation of Ref. [66] authors of Ref. [65] obtained for the six-loop RG series values of critical exponents which are quite in a good agreement with the other estimates (see table III). However the estimates of the fixed point coordinates differ essentially in different calculation schemes. It leads to the conclusion [65] that probably the optimal truncation of the RIM β -functions corresponds to a shorter series than a six-loop one.

VII. CONCLUSIONS

In the present article we have reviewed results obtained so far in the description of critical properties of a three dimensional weakly diluted quenched Ising model (RIM). Following the prevailing bulk of experimental, Monte-Carlo, and theoretical studies we focused our attention on critical exponents of the model. It can be seen from the number of relevant papers that the precise determination of the values of the exponents was a challenge justifying the scientific effort. The reason for this is two-fold. (i) The RIM allows to include in a simple model the macroscopic effects of disorder always present in real substances. (ii) The study of the influence of disorder on universal properties of critical behaviour besides practical needs is of high academic interest. It is the domain very close to critical temperature where even a very small amount of impurities can change the properties drastically in comparison with an ideal magnet. In accordance with the heuristic Harris criterion [71], only when the ideal system specific heat is divergent at criticality, the disordered magnet is characterized by new critical exponents. The change of critical exponents of RIM is well established in experimental as well as Monte-Carlo and theoretical studies. However, the numerical values obtained show much worse self-consistency compared with the situation in studies of pure Ising magnets. This happens due to both technical and principal difficulties. Moreover, often the technical difficulties in determination of the RIM exponents are related to the principal ones!

Though it is commonly believed that various defects are inevitable in experimental samples, the number of experimental RIM studies is much less than those devoted to the determination of the Ising model critical exponents. As an explanation one might mention that the Ising model universality class includes not only magnets but also simple fluids, ferroelectrics, binary alloys, etc. Moreover the RIM itself can show an effective critical behaviour of the same type as the behaviour in the Ising model universality class (!). The data for experimentally determined RIM critical exponents are collected in table I. As an peculiarity it is interesting to note that already in early studies [4] critical behaviour different from the pure Ising model has been observed. Surprisingly enough, since this work neither the experimental precision of the determination of the critical exponents has increased nor a narrower temperature interval around the critical point could be accessed. This can be explained by noting that starting from the end of eighties the researchers' attention shifted to random-field Ising model and the data for RIM were obtained only as side product results. It is worthwhile to note that the theoretically predicted critical exponents for quenched disorder [65]: $\nu \simeq 0.678, \gamma \simeq 1.330$ and for annealed disorder [145]: $\nu \simeq 0.708, \gamma \simeq 1.391$, are different but only by a small amount. Most probably, in real samples one encounters intermediate situations and exact coincidence between experiments on diluted crystalline antiferromagnets and theoretical calculations is hardly expected.

While the existence of a new universality class for the RIM has been observed already in early experimental studies, this was not the case in Monte-Carlo simulations. Due to the lack of a proper finite size analysis a continuous dependence of the critical exponents on concentration was observed. The exponents were interpreted as effective critical exponents [68,69]. In the following it was crucial to recognize the role of the correction-to-scaling exponent in the analysis of the simulation data [33–35]. This allowed to conclude from the numerical data on the concentration-independent asymptotic critical exponents [33]. As one can note from the table II the improvement of computers as well as of the calculation algorithms allowed to increase the accuracy of critical exponents. Recently in Monte-Carlo simulations of the RIM attention was paid also to study of the problems of self-averaging in diluted systems [37,38].

The results of experimental studies and Monte-Carlo simulations are confirmed by theoretical calculations. The numerical values of critical exponents obtained by different theoretical methods are collected in the table III. Note, that all theoretical results were obtained within renormalization-group approach, and most of them within its field-theoretical formalism on the basis of the effective Landau-Ginzburg-Wilson Hamiltonian (8). Though the last approach encounters intrinsic obstacles such as problems with the breakdown of replica symmetry and the possible existence of Griffiths phase [80], it remains the only method which can calculate the asymptotic values of exponents. For the pure Ising model many results are also based on other methods such as high- and low-temperature expansions.

Another evident difference of the RIM in comparison with the Ising model lies in the applicability of different

regularisation schemes of field-theoretical renormalization-group approach. In the case of Ising model both massive and minimal subtraction scheme followed by ε -expansion provide consistent and reliable results. For the RIM, the ε -expansion degenerates into $\sqrt{\varepsilon}$ -expansion [43,45,58,61] which seems to be of no use for quantitative studies [59,63]. Moreover, the initial series in the couplings, both in the massive and the minimal subtraction schemes, seem not to be Borel summable [135,136,138]. Nevertheless, Padé-Borel-like resummation procedures have been employed and allowed to obtain convergent sequences for the critical exponents from low order series. This is evident from the agreement of the theoretical results obtained in different orders of perturbation theory (table III) with the data of experimental (table I) and Monte-Carlo (table II) studies. However, the resummation failed in higher orders which resulted in the conjecture that there exists an optimal truncation for the RIM RG functions [63].

On the basis of the six-loop RG functions of the massive schemes result could only be obtained [65] by means of a highly sophisticated resummation procedure [138]. In the frames of this scheme, the estimates for critical exponents are characterized by the same order of accuracy as for the Ising model, which are based [74] on six-loop expansions for RG β -functions and seven-loop for γ -functions. However, the determination of error-bars in the theoretical calculations is a difficult problem which is solved in various ways [62,65]. Here, the error-bars seem to measure rather uncertainty of specific theoretical procedures than the confidence intervals of true values.

For a comparison of the theoretical predictions with experimental and simulation data one should use effective critical exponents which have been calculated for the RIM within the RG approach [57,63].

At the very end of this review we want to attract attention again to the fact that the new critical behaviour corresponding to the RIM universality class was experimentally observed so far only in magnetic systems like (anti)ferromagnets (see Table I). Still it remains a challenge to set up an experiment showing RIM-behaviour in other condensed matter systems. A promising example might be a fluid near its liquid-gas critical point in a porous medium. Recently, precise experiments on the critical behaviour of liquid helium-4 near the superfluid transition in porous medium [146] confirmed the irrelevancy of quenched disorder. This was expected from the Harris criterion [147] since the specific heat exponent near the superfluid transition is roughly zero. Thus an experimental study of a simple liquid in a porous medium may provide the first observation of a RIM critical behaviour in a non-magnetic system [148].

ACKNOWLEDGEMENTS

Writing this review and performing studies of RIM we benefited from discussions and contacts with numerous colleagues. We greatly acknowledge useful discussions with: David Belanger, Bertrand Berche, Christian von Ferber, Hagen Kleinert, Victor Martín-Mayor, Alan McKane, Verena Schulte-Frohlinde, Mykola Shpot, Aleksandr Sokolov. The materials presented here were used in part during lectures given by one of us in summer semester 2001 in the Université Henri Poincaré, Nancy 1 (France). Yu.H expresses his thanks to Bertrand Berche and colleagues at the Laboratoire de physique des matériaux (Université Nancy 1) for their hospitality, support and many useful comments.

Work was supported in part by “Österreichische Nationalbank Jubiläumsfonds” through the grant No 7694.

-
- [1] For reviews see e.g. Stinchcombe R B, in *Phase Transitions and Critical Phenomena* (Eds C. Domb, J. L. Lebowitz) (New York: Academic, 1983), **7** and Ref. [2].
 - [2] Belanger D P *cond-mat/0009029* (to be published in the Brazilian Journal of Physics)
 - [3] For the recent MC results of RIM dynamic critical behaviour as well as their discussion in comparison with the theoretical data see: Parisi G, Ricci-Tersenghi F, Ruiz-Lorenzo J J *Phys. Rev. E* **60** 5198 (1999)
 - [4] Dunlap R A, Gottlieb A M *Phys. Rev. B* **23** 6106 (1981)
 - [5] Birgeneau R J, Cowley R A, Shirane G, Joshizawa H, Belanger D P King A R, Jaccarino V *Phys. Rev. B* **27** 6747 (1983)
 - [6] Hastings J M, Corliss L M, Kunnmann W *Phys. Rev. B* **31** 2902 (1985)
 - [7] Belanger D P, King A R, Jaccarino V *Phys. Rev. B* **34** 452 (1986)
 - [8] Barrett P H *Phys. Rev. B* **34** 3513 (1986)
 - [9] Mitchell P W, Cowley R A, Yoshizawa H, Böni P, Uemura Y J, Birgeneau R J *Phys. Rev. B* **34** 4719 (1986)
 - [10] Thurston T R, Peters C J, Birgeneau R J, Horn P M *Phys. Rev. B* **37** 9559 (1988)
 - [11] Rosov N, Kleinhammes A, Lidbjörk P, Hohenemser C, Eibschütz M *Phys. Rev. B* **37** 3265 (1988)
 - [12] Belanger D P, King A R, Ferreira I B, Jaccarino V *Phys. Rev. B* **37** 226 (1988)
 - [13] Ramos C A, King A R, Jaccarino V *Phys. Rev. B* **37** 5483 (1988)

- [14] Ferreira I B, King A R, Jaccarino V *Phys. Rev. B* **43** 10797 (1991)
- [15] Belanger D P, Wang J, Slanić Z, Han S-J, Nicklow R M, Lui M, Ramos C A, Lederman D *Journ. Magn. Magn. Mater.* **140-144** 1549 (1995)
- [16] Belanger D P, Wang J, Slanić Z, Han S-J, Nicklow R M, Lui M, Ramos C A, Lederman D *Phys. Rev. B* **54** 3420 (1996)
- [17] Hill J P, Feng Q, Harris Q J, Birgeneau R J, Ramirez A P, Cassanho A *Phys. Rev. B* **55** 356 (1997)
- [18] Slanić Z, Belanger D P *J. Magn. Magn. Mater.* **186** 65 (1998)
- [19] Slanić Z, Belanger D P, Fernandez-Baca J A *J. Magn. Magn. Mater.* **177-181** 171 (1998)
- [20] Slanić Z, Belanger D P *Phys. Rev. Lett.* **82** 426 (1999)
- [21] Landau D P *Phys. Rev. B* **22** 2450 (1980)
- [22] Marro J, Labarta A, Tejada J *Phys. Rev. B* **34** 347 (1986)
- [23] Chowdhury D, Stauffer D *J. Stat. Phys.* **44** 203 (1986)
- [24] Braun P, Fähnle M *J. Stat. Phys.* **52** 775 (1988)
- [25] Braun P, U. Staaßen, T. Holey, M. Fähnle *Int. J. Mod. Phys. B* **3** 1343 (1989)
- [26] Wang J-S, Chowdhury D *J. Phys. France* **50** 2905 (1989)
- [27] Wang J-S, Wöhlert M, Mühlenbein H, Chowdhury D *Physica A* **166** 173 (1990)
- [28] Holey T, Fähnle M *Phys. Rev. B* **41** 11709 (1990); Fähnle M, Holey T, Eckert J *J. Magn. Magn. Mat.* **104-107** 195 (1992)
- [29] Heuer H-O *Europhys. Lett.* **12** 551 (1990); Heuer H-O *Phys. Rev. B* **42** 6476 (1990)
- [30] Heuer H-O *J. Phys. A* **26** L333 (1993)
- [31] Prudnikov V V, Vakilov A N *JETF (in Russian)* **103** 962 (1993)
- [32] Hennecke M *Phys. Rev. B* **48** 6271 (1993)
- [33] Ballesteros H G, Fernández L A, Martín-Mayor V, Muñoz Sudupe A, Parisi G, Ruiz-Lorenzo J J *Phys. Rev. B* **58** 2740 (1998)
- [34] Wiseman S, Domany E *Phys. Rev. Lett.* **81** 22 (1998)
- [35] Wiseman S, Domany E *Phys. Rev. E* **58** 2938 (1998)
- [36] Aharony A, Harris A B, Wiseman S *Phys. Rev. Lett.* **81** 252 (1998)
- [37] Marqués M I, Gonzalo J A *Physica A* **284** 187 (2000)
- [38] Marqués M I, Gonzalo J A *Phys. Rev. E* **60** 2394 (1999)
- [39] Marqués M I, Gonzalo J A, Íñiguez J *Phys. Rev. E* **62** 191 (2000)
- [40] Hukushima K *J. Phys. Soc. Jap.* **69** 631 (2000)
- [41] Berche P E, Chatelain C, Berche B Janke W, in *MECO25, Middle European Cooperation in Statistical Physics* (Pont-à-Mousson: France, 2000) p. 51.
- [42] Harris A B, Lubensky T C *Phys. Rev. Lett.* **33** 1540 (1974)
- [43] Khmel'nitskii D E *Zh. Eksp. Teor. Fiz.* **68** 1960 (1975) [*Sov. Phys. JETP* **41** 981]
- [44] Lubensky T C *Phys. Rev. B* **11** 3573 (1975)
- [45] Grinstein G, Luther A *Phys. Rev. B* **13** 1329 (1976)
- [46] Jayaprakash C, Katz H J *Phys. Rev. B* **16** 3987 (1977)
- [47] Shalaev B N *Zh. Eksp. Teor. Fiz.* **73** 2301 (1977) [*Sov. Phys. JETP* **46** 1204]
- [48] Sokolov A I *Fiz. Tv. Tela* **19** 748 (1977) [*Sov. Phys. - Solid State* **19** 433]
- [49] Sokolov A I, Shalaev B N *Fiz. Tv. Tela* **23** 2058 (1981) [*Sov. Phys. - Solid State* **23** 1200]
- [50] Newman K E, Riedel E K *Phys. Rev. B* **25** 264 (1982)
- [51] Jug J *Phys. Rev. B* **27** 609 (1983)
- [52] Mayer I O, Sokolov A I *Fiz. Tv. Tela* **26** 3454 (1984) [*Sov. Phys. - Solid State* **26** 2076]
- [53] Shpot N A *Phys. Lett. A* **142** 474 (1989)
- [54] Mayer I O, Sokolov A I, Shalaev B N *Ferroelectrics* **95** 93 (1989)
- [55] Mayer I O *J. Phys. A* **22** 2815 (1989)
- [56] Holovatch Yu, Shpot M *J. Stat. Phys.* **66** 867 (1992)
- [57] Janssen H K, Oerding K, Sengespeick E *J. Phys. A* **28** 6073 (1995)
- [58] Shalaev B N, Antonenko S A, Sokolov A I *Phys. Lett. A* **230** 105 (1997)
- [59] Folk R, Holovatch Yu, Yavors'kii T *J. Phys. Stud.* **2** 213 (1998)
- [60] Holovatch Yu, Yavors'kii T *J. Stat. Phys.* **93** 785 (1998); *Cond. Mat. Phys.* iss 11 87 (1997)
- [61] Folk R, Holovatch Yu, Yavors'kii T *Pis'ma v ZhETF* **69** 698 (1999) [*JETP Letters* **69** 747]
- [62] Varnashev K B *Phys. Rev. B* **61** 14660 (2000)
- [63] Folk R, Holovatch Yu, Yavors'kii T *Phys. Rev. B* **61** 15114 (2000)
- [64] Pakhmin D V, Sokolov A I *Pis'ma v ZhETF* **71** 600 (2000) [*JETP Letters* **71** 412]; Pakhmin D V, Sokolov A I *Phys. Rev. B* **61** 15130 (2000)
- [65] Pelissetto A, Vicari E *Phys. Rev. B* **62** 6393 (2000)
- [66] Carmona J M, Pelissetto A, Vicari E *Phys. Rev. B* **61** 15136 (2000)
- [67] See e.g.: Stanley H E *Introduction to Phase Transitions and Critical Phenomena* (Oxford: Clarendon Press 1971)
- [68] Kouvel J S, Fisher M E *Phys. Rev.* **136** A1626 (1964)

- [69] Riedel E K, Wegner F J *Phys. Rev. B* **9** 294 (1974)
- [70] Wegner F J *Phys. Rev. B* **5** 4529 (1972)
- [71] Harris A B *J. Phys. C* **7** 1671 (1974)
- [72] Chayes J T, Chayes L, Fisher D S, Spenser T *Phys. Rev. Lett.* **57** 2999 (1986)
- [73] We give here recent renormalization group estimates for the critical exponents of the pure three dimensional Ising model obtained from the resummation of perturbation theory series of a scalar $d = 3$ ϕ^4 theory [74].
- [74] Guida R, Zinn-Justin J *J. Phys. A* **31** 8103 (1998)
- [75] Emery V J *Phys. Rev. B* **11** 239 (1975); Edwards S F, Anderson P W *J. Phys. F* **5** 965 (1975)
- [76] Brout R *Phys. Rev.* **115** 824 (1959)
- [77] Fisher M E *Phys. Rev.* **176** 257 (1968)
- [78] Dotsenko V, Harris A B, Sherrington D, Stinchcombe R B *J. Phys. A* **28** 3093 (1995)
- [79] Dotsenko V S *preprint cond-mat/9809097* (1998)
- [80] Griffiths R B *Phys. Rev. Lett.* **23** 17 (1969)
- [81] Dotsenko V, Feldman D E *J. Phys. A* **28** 5183 (1995)
- [82] Wu X t *Physica A* **251** 309 (1998)
- [83] Prudnikov V V, Prudnikov P V, Fedorenko A A *J. Phys. A* **34** L145 (2001)
- [84] See chapter V for a more detailed review.
- [85] Hutchings M T, Schulhof M P, Gugenheim H J *Phys. Rev. B* **5** 154 (1972)
- [86] Hutchings M T, Rainford B D, Gugenheim H J *J. Phys. C* **3** 307 (1970)
- [87] Heller P *Phys. Rev.* **146** 403 (1966)
- [88] Dietrich O *J. Phys. C* **2** 2022 (1969)
- [89] Schullhof M P, Nathans R, Heller P, Linz A *Phys. Rev. B* **1** 2304 (1969)
- [90] Wertheim G K, Buchanan D N E *Phys. Rev.* **161** 478 (1967)
- [91] Belanger D P, King A R, Jaccarino V *J. Appl. Phys.* **53** 2704 (1982)
- [92] Meyer G M, Dietrich O W *J. Phys. C* **11** 1451 (1978)
- [93] Cowley R A, Carneiro K *J. Phys. C* **13** 3281 (1980)
- [94] Belanger D P, Borsa F, King A R, Jaccarino V *J. Magn. Magn. Mater.* **15-18** 807 (1980)
- [95] Gehring G A *J. Phys. C* **10** 531 (1977)
- [96] Fishman S, Aharony A *J. Phys. C* **12** L729 (1979)
- [97] Cardy J *Phys. Rev. B* **29** 505 (1984)
- [98] Belanger D P, Young A P *J. Mag. Mag. Mater.* **100** 272 (1991)
- [99] Belanger D P, Lui M, Erwin R W *Mat. Res. Soc. Symp. Proc.* **313** (1993) 755
- [100] Goldman A I, Mohanty K, Shirane G, Horn P M, Green R L, Peters C J, Thurston T R, Birgeneau R J *Phys. Rev. B* **36** 5609 (1987)
- [101] *Monte Carlo methods in Statistical Physics* (Ed K Binder) (Berlin: Springer, 1979)
- [102] Berche B, unpublished.
- [103] Barber M N, Pearson R B, Toussaint D, Richardson J L *Phys. Rev. B* **32** 1720 (1985)
- [104] Swedsen R H, Wang J S *Phys. Rev. Lett.* **58** 86 (1987); Wolff U *Phys. Lett.* **228B** 379 (1989)
- [105] Heuer H-O *Comput. Phys. Commun.* **59** 387 (1990)
- [106] Wiseman S, Domany E *Phys. Rev. E* **52** 3469 (1995)
- [107] Aharony A, Harris A B *Phys. Rev. Lett.* **77** 3700 (1996)
- [108] Weinrib A, Halperin B I *Phys. Rev. B* **27** 413 (1983)
- [109] Currently two possible scenarios for the influence of long-range-correlated disorder on critical behaviour are discussed (c.f. Refs [108] and [110]). Although both confirm the relevance of long-range-correlated disorder, they lead to different numerical predictions for the critical exponents.
- [110] Prudnikov V V, Prudnikov P V, Fedorenko A A *J. Phys. A* **32** L399 (1999); *J. Phys. A* **32** 8587 (1999); *Phys. Rev. B* **62** 8777 (2000); Blavats'ka V, von Ferber C, Holovatch Yu *J. Mol. Liq.* **91** 77 (2001); *Phys. Rev. E* (submitted).
- [111] Brézin E, Le Guillou J C, Zinn-Justin J in *Phase Transitions and Critical Phenomena* (Eds C Domb, M S Green) **6** (London: Academic Press, 1976); Amit D J *Field Theory, the Renormalization Group, and Critical Phenomena* (Singapore: World Scientist, 1989)
- [112] Zinn-Justin J *Quantum Field Theory and Critical Phenomena (International Series of Monographs on Physics, 92)* (Oxford Univ Press, 1996); Kleinert H, Schulte-Frohlinde V *Critical Properties of ϕ^4 -Theories* (Singapore: World Scientific, 2001); Pelissetto A, Vicari E, *preprint cond-mat/0012164* (2000)
- [113] 't Hooft G, Veltman M *Nucl. Phys. B* **44** 189 (1972); 't Hooft G *Nucl. Phys. B* **61** 455 (1973)
- [114] Parisi G in: *Proceedings of the Cargrèse Summer School* (unpublished, 1973); Parisi G *J. Stat. Phys.* **23** 49 (1980)
- [115] Vladimirov V S *Uravneniia matematicheskoi fiziki* (Moscow: Nauka, 1976)
- [116] Nasser I, Folk R *Phys. Rev. B* **52** 15799 (1995)
- [117] Frey E, Schwabl F *Phys. Rev. B* **42** 8261 (1990)
- [118] Kleinert H, Schulte-Frohlinde V *Phys. Lett. B* **342** 284 (1995)
- [119] Bervillier C, Shpot M *Phys. Rev. B* **46** 955 (1992)

- [120] Mayer I *Physica A* **252** 450 (1998)
- [121] Values of the loop integrals for fixed space dimension $d = 2$, $d = 3$ are given in: Nickel B G, Meiron D I, Baker G A *Compilation of 2pt and 4pt graphs for continuous spin model* (University of Guelph Report, 1977)
- [122] Holovatch Yu, Krokmal's'kii T *J. Math. Phys.* **35** 3866 (1994)
- [123] Wilson K G, Fisher M E *Phys. Rev. Lett.* **28** 240 (1972)
- [124] Schloms R, Dohm V *Europhys. Lett.* **3** 413 (1987); Schloms R, Dohm V *Nucl. Phys. B* **328** 639 (1989)
- [125] Pseudo- ε expansion was introduced by B.G. Nickel, (unpublished), see Ref. [19] in Ref. [126]. For an application of the pseudo- ε expansion technique in models with several couplings see: von Ferber C, Holovatch Yu *Europhys. Lett.* **39** 31 (1997); *Phys. Rev. E* **56** 6360 (1997); **59** 6914 (1999), and Folk R, Holovatch Yu, Yavors'kii T *Phys. Rev. B* **62** 12195 (2000)
- [126] Le Guillou J C, Zinn-Justin J *Phys. Rev. B* **21** 3976 (1980)
- [127] Newlove S A *J. Phys. C* **16** L423 (1983)
- [128] Shpot N A *Zh. Eksp. Teor. Fiz.* **98** 1762 (1990) [*Sov. Phys. JETP* **71** 989]
- [129] Folk R, Holovatch Yu in: *Correlations, Coherence, and Order* (Eds D V Shopova, D I Uzunov) (N.Y.-London: Kluwer Academic/Plenum Publishers, 1999) p. 83
- [130] Hardy G H *Divergent Series* (Oxford, 1948)
- [131] Eckmann J-P, Magnen J, Seneor R *Commun. Math. Phys.* **39** 251 (1975)
- [132] Lipatov L *Sov. Phys. JETP.* **45** 216 (1977)
- [133] Brézin E, Le Guillou J, Zinn-Justin J *Phys. Rev. D* **15** 1544 (1977)
- [134] Brézin E, Parisi G *J. Stat. Phys.* **19** 269 (1978)
- [135] Bray A J, McCarthy T, Moore M A, Reger J D, Young A P *Phys. Rev. B* **36** 2212 (1987)
- [136] McKane A J *Phys. Rev. B* **49** 12003 (1994)
- [137] Baker G A, Nickel B G, Green M S, Meiron D I *Phys. Rev. Lett.* **36** 1351 (1976)
Baker G A, Nickel B G, Meiron D I *Phys. Rev. B* **17** 1365 (1978)
- [138] Álvarez G, Martín-Mayor V, Ruiz-Lorenzo J J *J. Phys. A* **33** 841 (2000)
- [139] Baker G A, Jn, Graves-Morris P *Padé Approximants* (Addison-Wesley: Reading, MA, 1981)
- [140] Watson P J S *J. Phys. A* **7** L167 (1974)
- [141] Chisholm J S R Rational approximants defined from double power series *Math. Comp.* **27** 841 (1973)
- [142] Folk R, Holovatch Yu, Yavors'kii T, unpublished
- [143] Zinn-Justin J, *Phys. Rep.* **70** 109 (1981)
- [144] Holovatch Yu *Lectures on Critical Phenomena: Polymers, Diluted Systems, Magnets* (Linz: unpublished, 1996)
- [145] These numbers follow from the Fisher renormalization (11) applied to the pure $d=3$ Ising model exponents (4).
- [146] Yoon J, Chan M H W *Phys. Rev. Lett.* **78** 4801 (1997); see also: Zassenhaus G M, Reppy J D *cond-mat/9907427* (1999)
- [147] Experimentally measured value of the heat capacity critical exponent at the λ -transition in helium-4 is $\alpha = -0.01285 \pm 0.00038$ [Lipa J A, Swanson D R, Nissen J A, Chui T C P, Israelsson U E *Phys. Rev. Lett.* **76** 944 (1996)] and therefore due to the Harris criterion weak quenched disorder should not influence the critical exponents.
- [148] Only in a special case liquids in porous media are an example for the site diluted Ising model; otherwise they are conjectured to be examples for random-field models [see e.g. Pitard E, Rosinberg M L, Stell G, Tarjus G *Phys. Rev. Lett.* **74** 4361 (1995)]

VIII. TABLES AND FIGURES

TABLE I. The experimentally measured critical exponents of the materials, which correspond to random Ising models. The measurement procedures are given in the following notations: NMR — nuclear magnetic resonance; LB — linear birefringence; NS — neutron scattering; MS — Mössbauer spectroscopy; SMXS — synchrotron magnetic x-ray scattering; XS — x-ray scattering; τ denotes the reduced temperature interval, where the power-law fit was done or the minimal value of the reduced temperature reached in an experiment.

Ref.	material	method	$ \tau $	β	γ	ν	α
Dunlap et al., 1981 Ref. [4]	$\text{Mn}_p\text{Zn}_{1-p}\text{F}_2$ $p=0.864$	NMR	10^{-3}	0.349 ± 0.008	—	—	—
Birgeneau et al., 1983 Ref. [5]	$\text{Fe}_p\text{Zn}_{1-p}\text{F}_2$ $p=0.6, 0.5$	NS; LB	$10^{-1} \div 2 \cdot 10^{-3}$ $2 \cdot 10^{-2} \div 2 \cdot 10^{-3}$	—	1.44 ± 0.06	0.73 ± 0.03	-0.09 ± 0.03
Hastings et al., 1985 Ref. [6]	$\text{Dy}_3\text{Al}_5\text{O}_{12}$ +1% Y powder	NS	$4 \cdot 10^{-2}$	0.350 ± 0.01	—	0.73	—
Belanger et al., 1986 Ref. [7]	$\text{Fe}_p\text{Zn}_{1-p}\text{F}_2$ $p = 0.46$	NS	$10^{-1} \div 1.5 \cdot 10^{-3}$	—	1.31 ± 0.03	0.69 ± 0.01	—
Barret, 1986 Ref. [8]	$\text{Fe}_p\text{Zn}_{1-p}\text{F}_2$ $p = 0.9925 \div 0.95$	MS	$(4.7 \div 36 \cdot 10^{-3}) \div 1 \cdot 10^{-3}$	0.36 ± 0.01	—	—	—
Mitchell et al., 1986 Ref. [9]	$\text{Mn}_p\text{Zn}_{1-p}\text{F}_2$ $p = 0.75$ $p = 0.5$ $p = 0.5$	NS	$2 \cdot 10^{-1} \div 4 \cdot 10^{-4}$ $1 \cdot 10^{-1} \div 5 \cdot 10^{-3}, \tau > 0$ $1 \cdot 10^{-1} \div 5 \cdot 10^{-3}, \tau < 0$	— — —	1.364 ± 0.076 1.57 ± 0.16 1.56 ± 0.16	0.715 ± 0.035 0.75 ± 0.05 0.76 ± 0.08	—
Thurston et al., 1988 Ref. [10]	$\text{Mn}_p\text{Zn}_{1-p}\text{F}_2$ $p = 0.5$	SMXS	$6 \cdot 10^{-2} \div 1 \cdot 10^{-3}$	0.33 ± 0.02	—	—	—
Rosov et al., 1988 Ref. [11]	$\text{Fe}_p\text{Zn}_{1-p}\text{F}_2$ $p = 0.9$	MS	$1 \cdot 10^{-1} \div 3 \cdot 10^{-4}$	0.350 ± 0.009	—	—	—
Ramos et al., 1988 Ref. [13]	$\text{Mn}_p\text{Zn}_{1-p}\text{F}_2$ $p = 0.40, 0.55, 0.83$	LB	$10^{-2}?$	—	—	—	-0.09 ± 0.03
Ferreira et al., 1991 Ref. [14]	$\text{Fe}_p\text{Zn}_{1-p}\text{F}_2$ $0.31 \leq p \leq 0.84$	LB	?	—	—	—	-0.09
Belanger et al., 1995 Ref. [15]	$\text{Fe}_p\text{Zn}_{1-p}\text{F}_2$ $p = 0.5$	NS	$< 10^{-1}$	0.35	—	—	—
Belanger et al., 1996 Ref. [16]	$\text{Fe}_p\text{Zn}_{1-p}\text{F}_2$ $p = 0.52$	NS	10^{-2}	0.35	—	—	—
Hill et al., 1997 Ref. [17]	$\text{Fe}_p\text{Zn}_{1-p}\text{F}_2$ $p = 0.5$	XS	10^{-2}	0.36 ± 0.02	—	—	—
Slanic et al., 1998 Ref. [18]	$\text{Fe}_p\text{Zn}_{1-p}\text{F}_2$ $p = 0.93$	LB	?	—	—	—	-0.10 ± 0.02
Slanic et al., 1998 Ref. [19]	$\text{Fe}_p\text{Zn}_{1-p}\text{F}_2$ $p = 0.93$	NS	?	—	1.35 ± 0.01	0.71 ± 0.01	—
Slanic et al., 1999 Ref. [20]	$\text{Fe}_p\text{Zn}_{1-p}\text{F}_2$ $p = 0.93$	NS	$10^{-2} \div 1.14 \cdot 10^{-4}$	—	1.34 ± 0.06	0.70 ± 0.02	—

TABLE II. The critical exponents of the RIM as they are obtained in MC simulations. The asterisk at concentration denotes that disorder was realized in a canonical manner.

Ref.	max. size	concentr. range	p	β	γ	ν
Landau, 1980 Ref. [21]	30	$0.4 < p \leq 1$	all	0.31	1.25	—
Marro et al., 1986 Ref. [22]	40	$0.8 \leq p \leq 1$	1	0.30 ± 0.02	—	—
			0.985	0.31 ± 0.02	—	—
			0.95	0.32 ± 0.03	—	—
			0.9	0.355 ± 0.010	—	—
			0.8	0.385 ± 0.015	—	—
Chowdhury et al., 1986 Ref. [23]	90	$0.8 \leq p \leq 1$	1	0.29 ± 0.02	—	—
			0.95	0.28 ± 0.02	—	—
			0.90	0.31 ± 0.02	—	—
			0.80	0.37 ± 0.02	—	—
Braun et al., 1988 Ref. [24]	40	—	0.80	0.392 ± 0.03	—	—
Wang et al., 1989 Ref. [26]	100	$0.4 \leq p \leq 0.8$	all	—	1.52 ± 0.07	0.77 ± 0.04
Wang et al., 1990 Ref. [27]	300	—	0.8	—	1.36 ± 0.04	—
Holey et al., 1990 Ref. [28]	64	$0.8 < p \leq 1$	1	—	—	$0.629(4)$
			0.9	—	—	$< 2/3$
			0.8	—	—	$0.688(13)$
Heuer, 1990 Ref. [29]	60	$0.5 < p \leq 1$	1	0.305 ± 0.01	1.24 ± 0.01	—
			0.9	0.315 ± 0.01	1.30 ± 0.01	—
			0.8	0.330 ± 0.01	1.35 ± 0.01	—
			0.6	0.330 ± 0.01	1.48 ± 0.02	—
			0.5	0.335 ± 0.01	1.49 ± 0.02	—
Heuer, 1993 Ref. [30]	60	$0.6 < p \leq 1$	1	0.33 ± 0.01	1.22 ± 0.02	0.624 ± 0.010
			0.95	0.31 ± 0.02	1.28 ± 0.03	0.64 ± 0.02
			0.9	0.31 ± 0.02	1.31 ± 0.03	0.65 ± 0.02
			0.8	0.35 ± 0.02	1.35 ± 0.03	0.68 ± 0.02
			0.6	0.33 ± 0.02	1.51 ± 0.03	0.72 ± 0.02
Hennecke et al., 1993 Ref. [32]	90	—	0.6	0.42 ± 0.04	—	0.78 ± 0.01
Wiseman et al., 1998 Ref. [34]	64	—	0.8	0.344 ± 0.003	1.357 ± 0.008	0.682 ± 0.003
Wiseman et al., 1998 Ref. [35]	90	—	0.6*	0.316 ± 0.013	1.522 ± 0.031	0.722 ± 0.008
	80	—	0.6	0.313 ± 0.012	1.508 ± 0.028	0.717 ± 0.007
Ballesteros et al., 1998 Ref. [33]	128	$0.4 \leq p \leq 0.9$	all	0.3546 ± 0.0028	1.342 ± 0.010	0.6837 ± 0.0053
Marques et al., 2000 Ref. [38]	60	$0.8 \leq p \leq 0.9975$	all	0.3546	1.342	—
Marques et al., 2000 Ref. [39]	100	0.5	—	—	—	0.6837

TABLE III. The theoretical values for asymptotic critical exponents of the RIM. n LA denotes the n th order in loopwise approximation within massive ('mass') and $3d$ minimal subtraction ('MS') schemes of field-theoretical renormalization group approach. The resummation procedures are given in the following notations: ChBr – Chisholm–Borel; PdBr – Padé–Borel; AW – ϵ algorithm of Wynn, CM – Borel transformation with conformal mapping. SF stands for Golner-Riedel scaling field approach, superscript c at the correction-to-scaling exponent ω indicates that the real part of corresponding complex number is shown.

Ref.	RG scheme	Order	Resummation	ν	η	γ	ω
Sokolov et al., 1981 Ref. [49]	mass	3LA	No		0.009	1.31	
Newman et al., 1982 Ref. [50]	SF	No		0.70	0.015	1.39	0.41
Jug, 1983 Ref. [51]	mass	2LA	ChBr	0.678	0.031	1.336	0.450 ^c
Mayer et al., 1984 Ref. [52]	mass	2LA 3LA	ChBr ChBr		0.031 0.022	1.337 1.325	
Mayer et al., 1989 Ref. [54]	mass	4LA	ChBr	0.670	0.034	1.326	
Mayer, 1989 Ref. [55]	mass	4LA 4LA	AW PdBr	0.6680 0.6714		1.318 1.321	
Shpot, 1989 Ref. [53]	mass	3LA	ChBr	0.671	0.021	1.328	0.359
Janssen et al., 1995 Ref. [57]	MS, 3d	3LA	PdBr	0.666		1.313	0.366
Holovatch et al, 1997 Ref. [60]	mass	3LA	ChBr	0.671	0.019	1.328	0.376
Folk et al., 1998 Ref. [59]	MS, 3d	2LA 3LA 4LA	ChBr	0.665 0.654 0.675	0.032 0.022 0.049	1.308 1.293 1.318	0.162 0.430 0.390 ^c
Folk et al., 1999 Ref. [61]	MS, 3d mass	4LA 4LA	ChBr ChBr				0.39(4) ^c 0.372(5)
Pakhnin et al., 2000 Ref. [64]	mass	5LA	PdBr	0.671(5)	0.025(10)	1.325(3)	0.32(6)
Varnashev, 2000 Ref. [62]	mass	4LA	PdBr PdBr	0.681(12) 0.672(4)	0.040(11) 0.034(10)	1.336(20) 1.323(10)	0.330
Pelissetto et al., 2000 Ref. [65]	mass	6LA	PdBr-CM PdBr-PdBr	0.678(10) 0.668(6)	0.030(3) 0.0327(19)	1.330(17) 1.313(14)	0.25(10) 0.25(10)

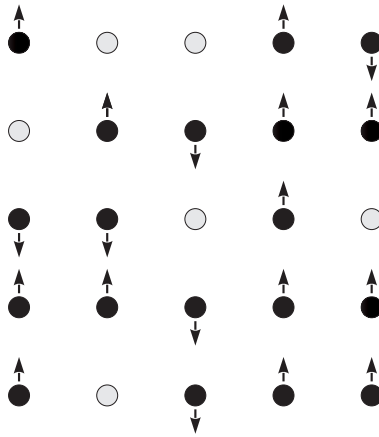


FIG. 1. Weakly diluted quenched 3d Ising model (random Ising model: RIM) describing a system of scalar "spins" randomly distributed in sites of a three-dimensional cubic lattice and fixed in certain positions.

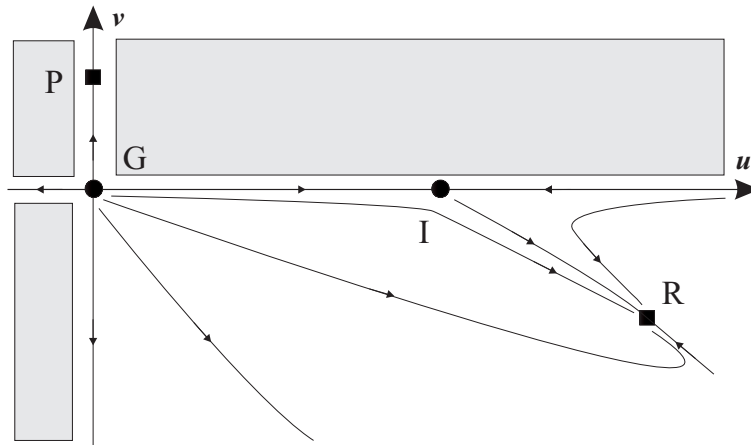


FIG. 2. RIM fixed points qualitative structure. Gaussian fixed point \mathbf{G} is stable for $d \geq 4$, stable fixed point \mathbf{P} can not be reached from the initial coupling values $u > 0, v < 0$ (this region as well as other unphysical for RIM regions are shown in grey tone), pure Ising fixed point \mathbf{I} is unstable whereas random fixed point \mathbf{R} is both stable and accessible (stable fixed points are shown by boxes).

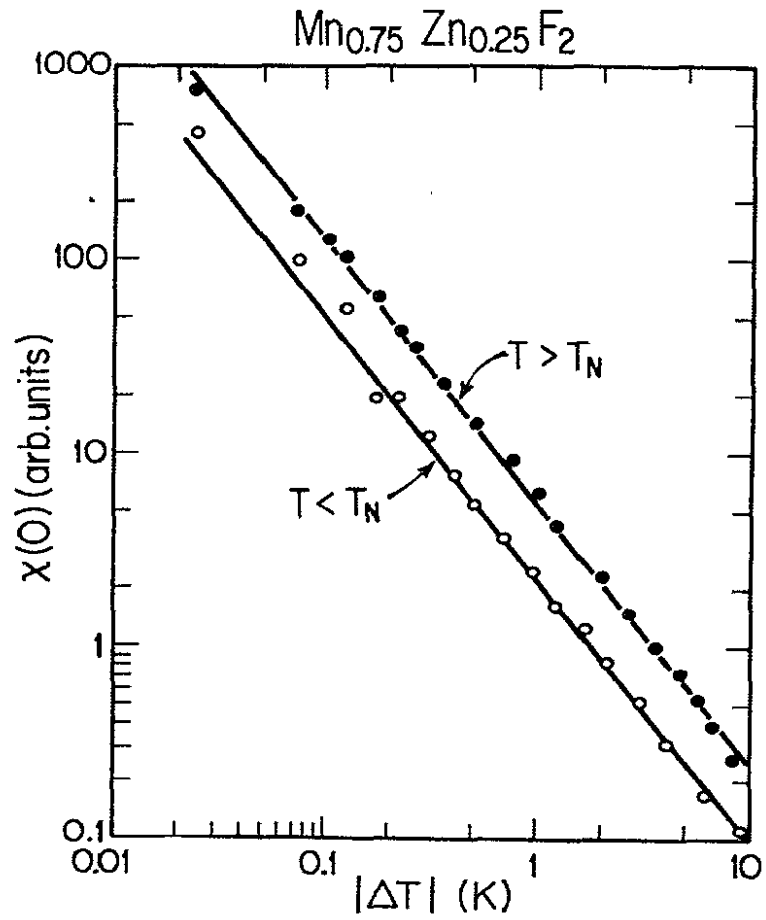


FIG. 3. Neutron scattering measurements of the susceptibility $\chi(0)$ in $\text{Mn}_{0.75}\text{Zn}_{0.25}\text{F}_2$ [9]. The solid lines are the results of fits to single power laws with exponents $\gamma \simeq 1.364$ above and below Néel temperature T_N . The critical behaviour is governed by RIM asymptotic critical exponents over the reduced temperature interval $4 \cdot 10^{-4} < |\tau| < 2 \cdot 10^{-1}$. The figure is taken from the Ref. [9].

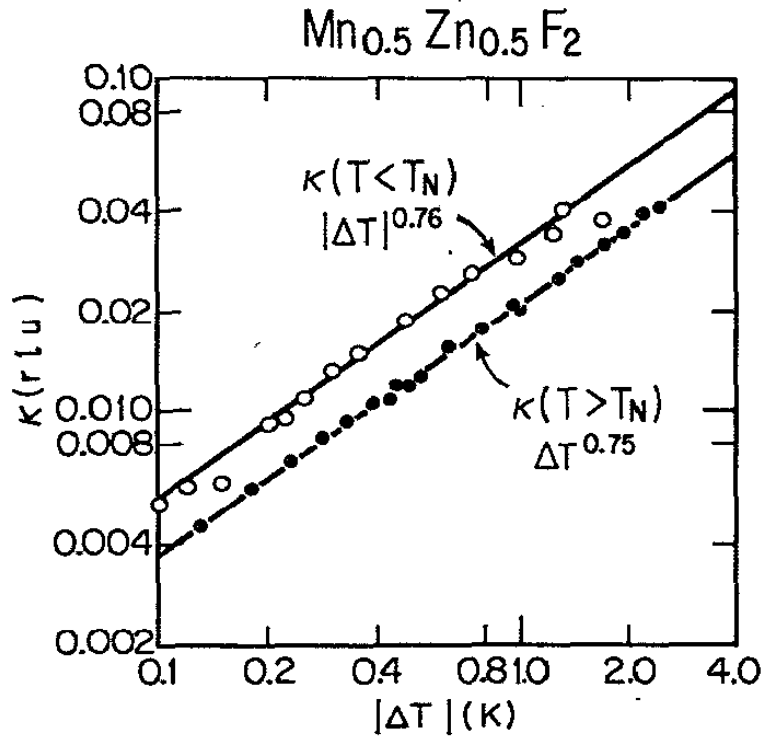


FIG. 4. Neutron scattering measurements of the longitudinal inverse correlation length κ in $\text{Mn}_{0.5}\text{Zn}_{0.5}\text{F}_2$ above and below T_N [9]. The solid lines are the results of fits to laws with the exponents $\nu' \simeq 0.76$ for $T < T_N$ and $\nu \simeq 0.75$ for $T > T_N$. The data give $\nu' = \nu$ within the errors (see Table I). The law holds in the reduced temperature interval $5 \cdot 10^{-3} < |\tau| < 10^{-1}$. The asymptotic region still is not reached as the observed effective exponents values show. The figure is taken from the Ref. [9].

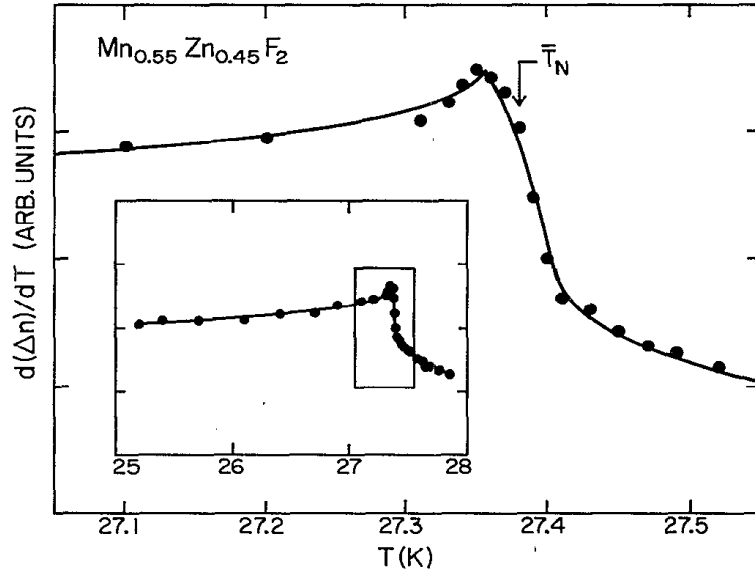


FIG. 5. The temperature derivative of the optical birefringence of $\text{Mn}_{0.55}\text{Zn}_{0.45}\text{F}_2$ at zero magnetic field. In the main part of the figure $d(\Delta n)/dT$ is shown for the critical region (indicated by box in the inset). The measurements bring about a cusp-like behaviour of the RIM specific heat with the critical exponent $\alpha = -0.09 \pm 0.03$. The figure is taken from Ref. [13].

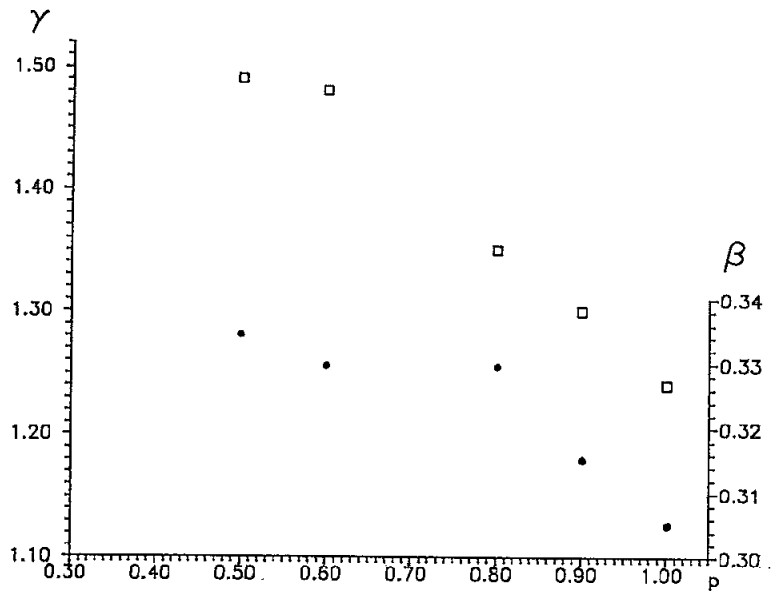


FIG. 6. Obtained in MC simulations [29] RIM effective critical exponents β (dots) and γ (squares) for different dilutions p . All exponents change continuously with dilution and are clearly different from their pure system values. The figure is taken from Ref. [29].

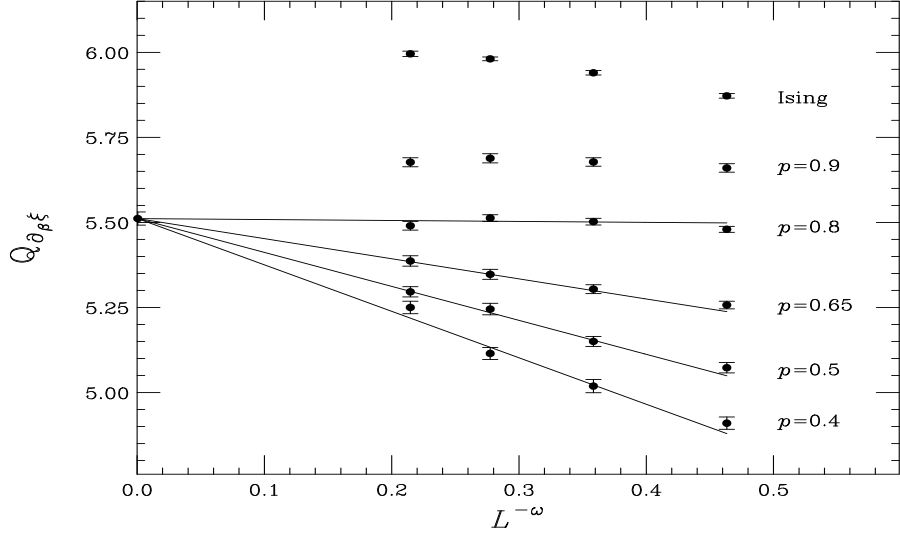


FIG. 7. Determination of the correction-to-scaling exponent ω in the MC simulations of Ref. [33]. Quantity $Q_{\partial\beta\xi} = 2^{1+1/\nu}$ is plotted for different dilutions $0.4 \leq p \leq 1$ and lattice sizes $8 \leq L \leq 128$. One can see that at $p = 0.9$ the system is crossing over from the pure Ising fixed point to the diluted one even for $L = 128$. The solid lines correspond to a fit $\omega = 0.37$ yielding the same infinite volume extrapolation for all $p \leq 0.8$. The figure is taken from Ref. [33].

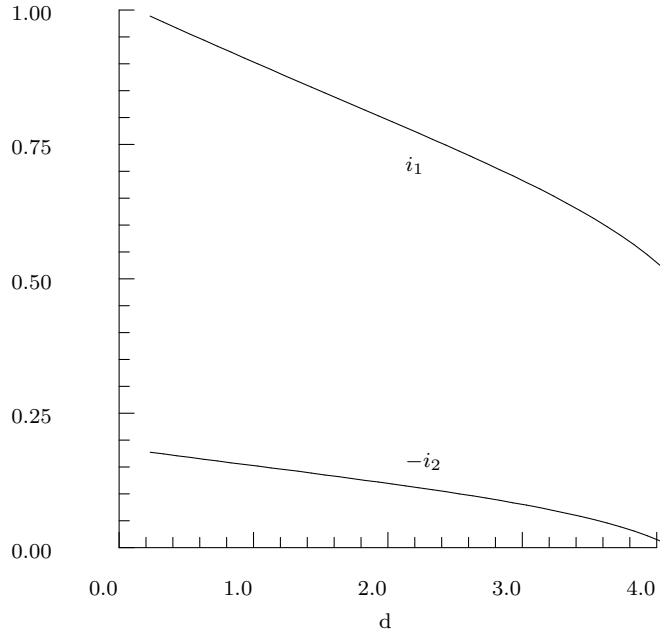


FIG. 8. Two-loop integrals of the RG functions in massive scheme (formulas (48)–(50)) as functions of space dimension d , Ref. [56].

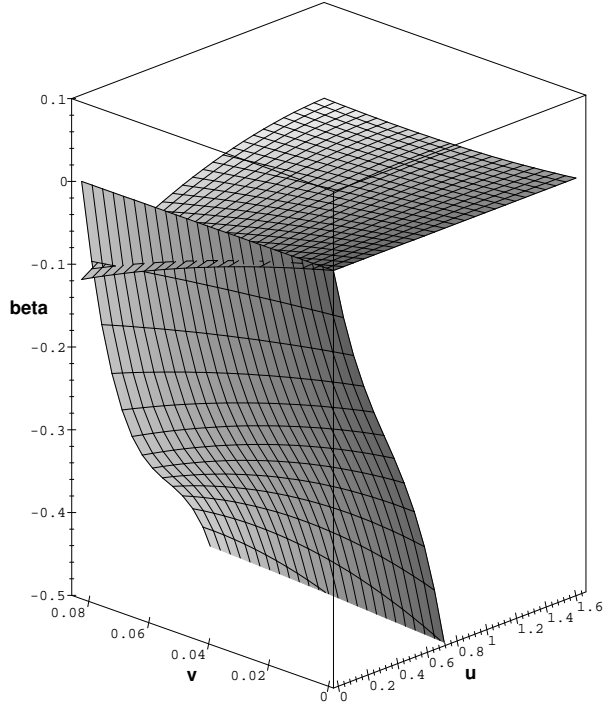


FIG. 9. β -functions of RIM $\beta_u(u, v)$, $\beta_v(u, v)$ calculated in two-loop approximation by a $d = 3$ minimal subtraction scheme without resummation. Only the Gaussian fixed point $u^* = v^* = 0$ survives. The figure is taken from Ref. [129].

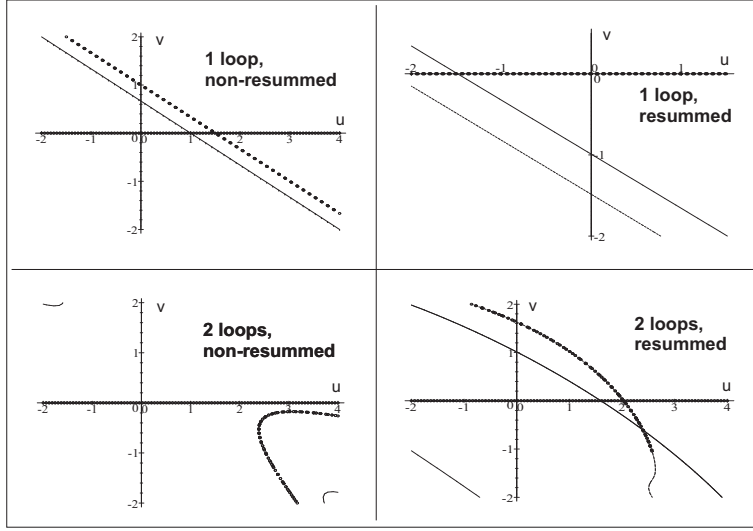


FIG. 10. The lines of zeros of non-resummed (left-hand column) and resummed by the Chisholm-Borel method (right-hand column) RIM massive β -functions in different orders of the perturbation theory: one- and two-loop approximations. Circles correspond to $\beta_u = 0$, thick lines depict $\beta_v = 0$. Thin solid and dashed lines show zeros of the analytically continued functions β_u and β_v respectively. One can see the appearance of the mixed fixed point $u > 0, v < 0$ in the two-loop approximation for the resummed β -functions. The figure is taken from Ref. [60].

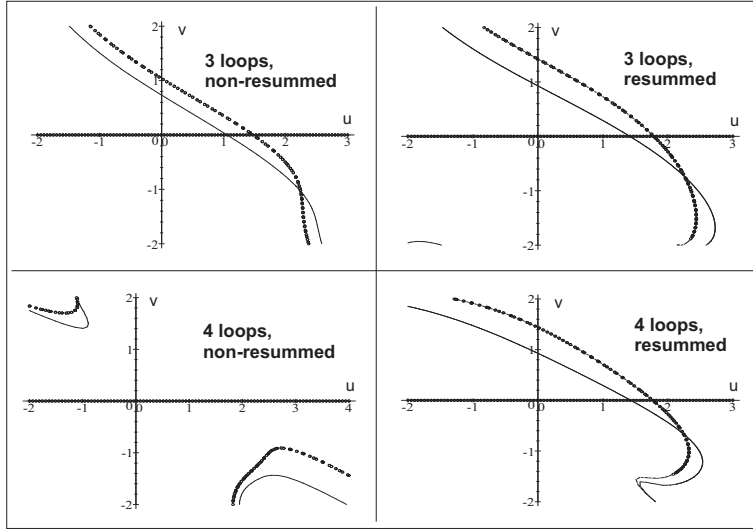


FIG. 11. The lines of zeros of non-resummed (left-hand column) and resummed by the Chisholm-Borel method (right-hand column) RIM massive β -functions in three- and four-loop approximations. The notations are the same as in the figure 10. Close to the mixed fixed point the behaviour of the resummed functions remains alike with the increase of the order of approximation. This is not the case for non-resummed functions. The figure is taken from Ref. [60].

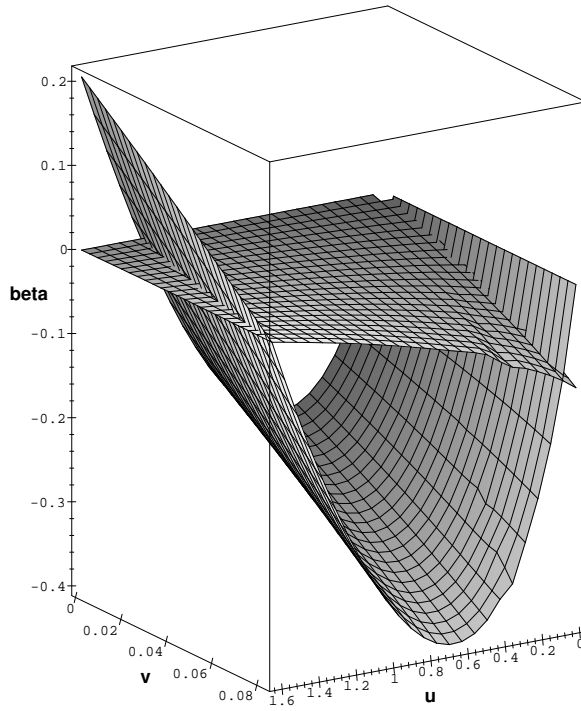


FIG. 12. Padé-Borel resummation technique applied to the β -functions of the figure 9. Resummation restores the presence of the fixed point $u^* \neq 0, v^* = 0$ and results in the appearance of a new stable fixed point $u^* \neq 0, v^* \neq 0$. The figure is taken from Ref. [129]. Note that the authors of Ref. [129] exploited different in comparison to formulas (40)-(43) normalization of couplings $u \rightarrow 3/2 u$ and $v \rightarrow -4 v$.

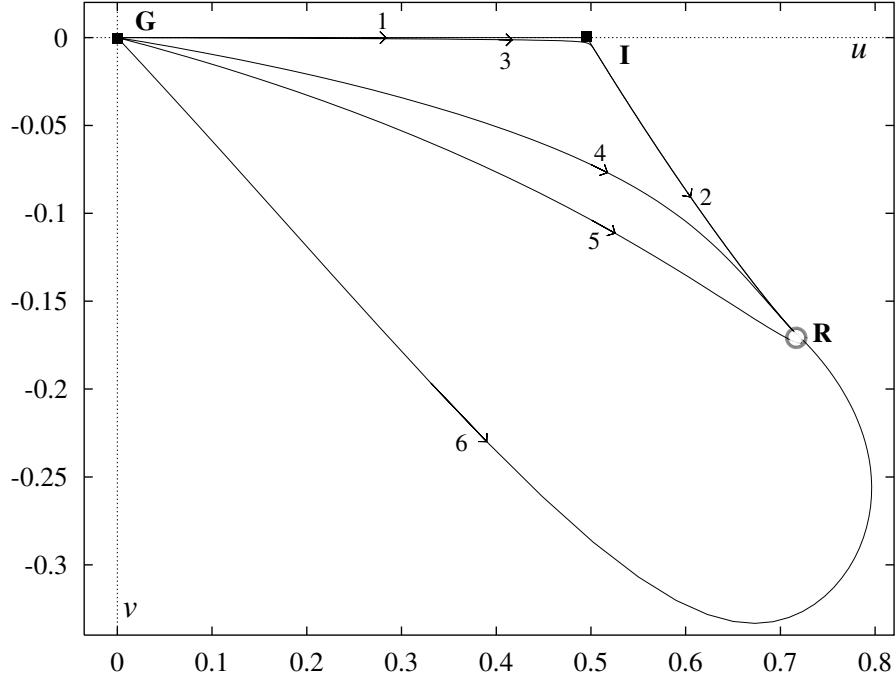


FIG. 13. Flow lines for the RIM. Fixed points G , I are unstable, fixed point R is the stable one. The figure is taken from Ref. [63]. Note that the authors of Ref. [63] exploited different in comparison to formulas (40)-(43) normalization of couplings $u \rightarrow 3u$ and $v \rightarrow 8/3v$.

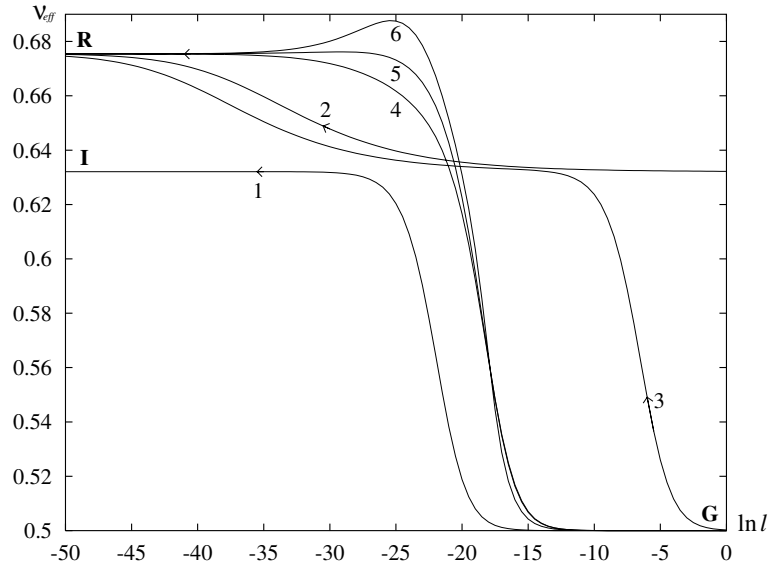


FIG. 14. Effective exponent ν_{eff} versus logarithm of the flow parameter ℓ for the flows shown in Fig. 13. The figure is taken from Ref. [63].

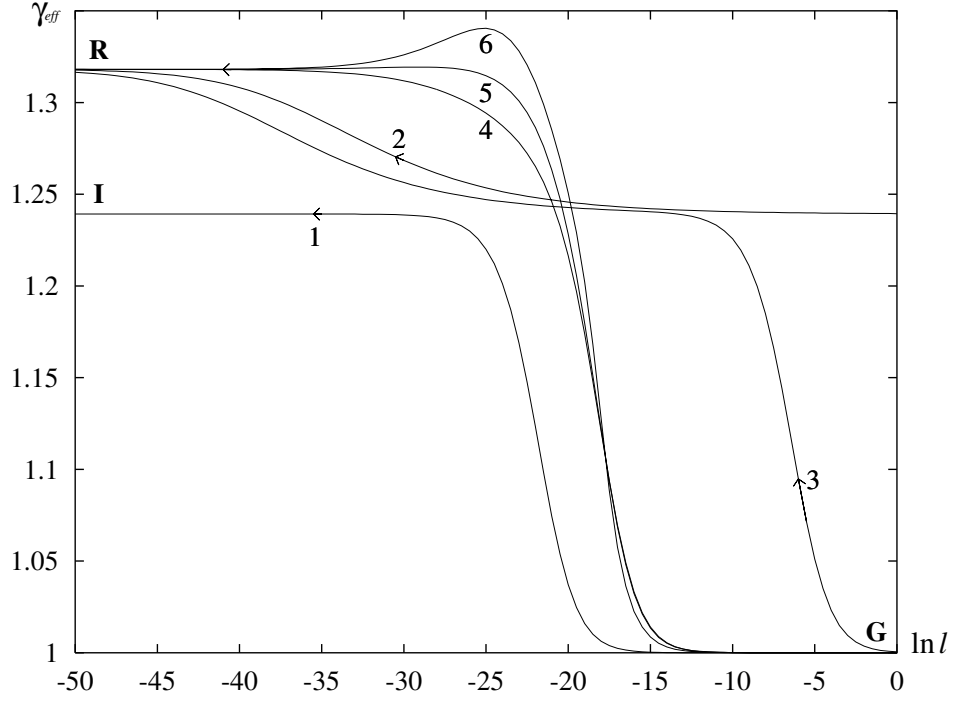


FIG. 15. Effective exponent γ_{eff} versus logarithm of the flow parameter ℓ for the flows shown in Fig. 13. The figure is taken from Ref. [63].

	0	1	2	3	4	5	6
0	-	-	-	-	-	-	-
1	-		±	-	-	-	
2	-	-	[62]	~	~		
3	[48,49]	[55,62]	[64]	~			
4	-	[64]	±	No approximant can be constructed			
5	-	~					
6	-						

FIG. 16. The fecundity of Padé–Borel resummation for the RIM β -functions in massive scheme. The numbers of a row M and of a column N correspond to a Padé approximant $[M/N]$ representing $(M+N)$ -loop approximation. Symbol “-” depicts that no fixed point values are available, “±” and “~” show that a method either uses analytic continuation due to poles on the real semi-axis or yields values very far from expected. The fruitful approximants are shown by dark colour and/or appropriate citations. Though working approximants are distributed rather stochastically, numerical results on their basis show evident convergence (table III).

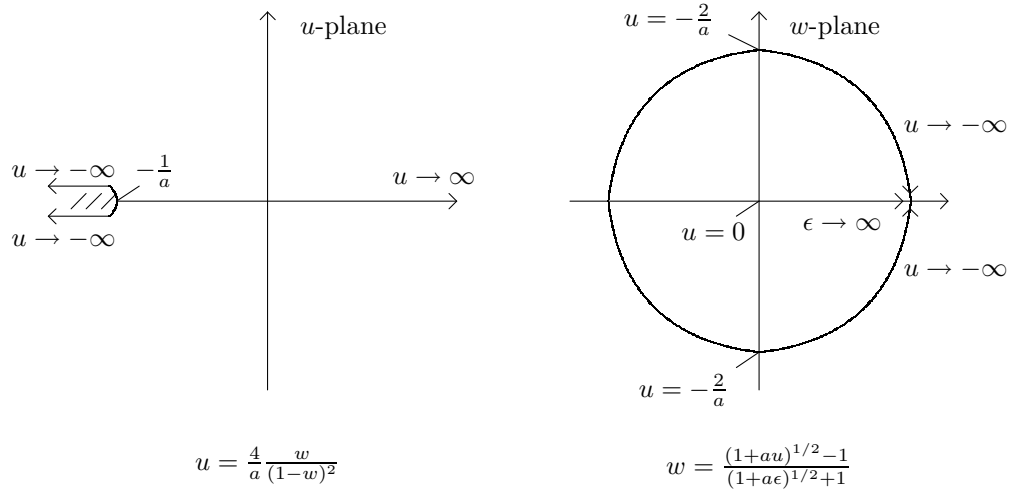


FIG. 17. Conformal mapping of the cut-plane onto a disc leaving the origin invariant, as prescribed by formulas (67). See the text for details. The figure is taken from Ref. [144].